



LAWRENCE
LIVERMORE
NATIONAL
LABORATORY

Accretion Timescale and Impact History of Mars Deduced from the Isotopic Systematics of Meteorites

L. E. Borg, S. J. K. Symes, G. A. Brennecka

July 8, 2014

Geochemica et Cosmochemica Acta

Disclaimer

This document was prepared as an account of work sponsored by an agency of the United States government. Neither the United States government nor Lawrence Livermore National Security, LLC, nor any of their employees makes any warranty, expressed or implied, or assumes any legal liability or responsibility for the accuracy, completeness, or usefulness of any information, apparatus, product, or process disclosed, or represents that its use would not infringe privately owned rights. Reference herein to any specific commercial product, process, or service by trade name, trademark, manufacturer, or otherwise does not necessarily constitute or imply its endorsement, recommendation, or favoring by the United States government or Lawrence Livermore National Security, LLC. The views and opinions of authors expressed herein do not necessarily state or reflect those of the United States government or Lawrence Livermore National Security, LLC, and shall not be used for advertising or product endorsement purposes.

Accretion Timescale and Impact History of Mars Deduced from the Isotopic Systematics of Meteorites

Lars E. Borg^{a*}, Steven J. K. Symes^b, Gregory A. Brennecke^a

a. Chemical Sciences Division, Lawrence Livermore National Laboratory, 7000 East Avenue L-231, Livermore CA 94550 USA.

b. Department of Chemistry, University of Tennessee-Chattanooga, Chattanooga, TN 37403, USA.

*Correspondence to: borg5@llnl.gov

Abstract

High precision Sm–Nd isotopic analyses have been completed on a suite of 11 martian basaltic meteorites in order to better constrain planetary differentiation processes on Mars. These data are used to better constrain the age of silicate differentiation of Mars and to evaluate the merits and disadvantages of various mathematical approaches that have been employed in previous work on this topic. Ages determined from the Sm–Nd isotopic systematics of individual samples are strongly dependent on the assumed Nd isotopic composition of the bulk planet. This assumption is problematic given differences observed between the Nd isotopic composition of Earth and chondritic meteorites and the fact that these materials are both commonly used to represent bulk planetary Nd isotopic compositions. Ages determined from ^{146}Sm – ^{142}Nd whole rock isochrons are less dependent on the assumed $^{142}\text{Nd}/^{144}\text{Nd}$ ratio of the planet, but require the sample suite to be derived from complementary, contemporaneously-formed source regions. In this work we develop a mathematical expression that defines the age of silicate differentiation based on the twin Sm–Nd decay chains that is independent of any *a priori* assumptions regarding the bulk isotopic composition of the planet. This expression is also applicable to mineral isochrons and has been used to successfully calculate ^{143}Nd – ^{142}Nd model crystallization ages of early refractory solids as well as lunar samples. When used in conjunction with high-precision Nd isotopic measurements completed on martian meteorites this expression yields an age of differentiation of the martian basaltic meteorite source regions of 4504 ± 5 Ma. Although Sm–Nd model ages of martian meteorites are commonly interpreted to record the age of planetary differentiation associated with magma ocean solidification, the young age determined here requires that either magma ocean solidification is a protracted process or there is an additional source of heat added to the martian interior. Recent thermal models suggest that Mars-sized bodies cool in only ~ 5 Ma after accretion ceases, even in the presence of a thick atmosphere. Thus, an extended period of accretion appears to be a reasonable mechanism to keep portions of the martian mantle partially molten until 4504 Ma. This heat source could either be associated with protracted accretion occurring at a quasi-steady state or alternatively associated with a late giant impact. This implies that accretion of Mars-sized bodies takes up to 60 Ma and is therefore likely to be contemporaneous with the initial stages of planetary differentiation associated with core formation. This challenges the concept that primordial

evolution of planets occurs in systems that are essentially closed, and may help to account for geochemical evidence implying addition of material into planetary interiors after core formation was completed.

1. INTRODUCTION

The planetesimal hypothesis is the favored model for explaining how terrestrial planets formed from the dust and gas that was present in the protoplanetary disk during the birth of our Solar System. This hypothesis describes how dust grains migrating toward the midplane of the disk accrete to form progressively larger planetesimals. Gravitational interactions between planetesimals produce a modest number of relatively large, Mars-sized, planetary embryos, which in turn randomly collide to form the terrestrial planets (Chambers, 2004). Accretion introduces significant quantities of heat into the newly forming terrestrial planets, resulting in broad scale melting and subsequent cooling. Elemental fractionation associated with melting and cooling are thought to produce mineralogically and chemically distinct reservoirs in the core, mantle, and crust resulting in primordial differentiation of the planet. Whereas isotopic dating of the earliest Solar System solids indicates that this process began at 4567 Ma (Amelin et al., 2002; Connelly et al., 2008), its duration is poorly defined.

The timescale of planetary differentiation is constrained by the systematics of daughter isotopes produced by short-lived radionuclide decay observed in planetary samples. Samples from the planet Mars are ideal for this purpose because they demonstrate obvious anomalies in key isotope systems, such as ^{182}Hf - ^{182}W and ^{146}Sm - ^{142}Nd . The suite of martian meteorites is comprised mostly of basalts, basaltic cumulates, and ultramafic rocks that have large systematic variations in trace element and isotopic compositions. The basaltic meteorites (shergottites) are the focus of this investigation. The inferred incompatible-element characteristics of the shergottite source regions have been used as a basis to divide the shergottites into subgroups called “enriched”, “depleted”, and “intermediate” (Symes et al., 2008). The initial Sr, Nd, and Hf isotopic systematics of the shergottites define mixing lines between incompatible-element enriched and incompatible-element depleted geochemical end-members (Borg et al., 2003; Borg and Draper, 2003) underscoring the close petrogenetic affinity between the shergottites. The second class of martian meteorites relevant to this investigation is the nakhlites. These meteorites are clinopyroxene cumulates with petrologic and geochemical characteristics that are nearly identical to one another. The nakhlites have ^{182}W isotopic compositions that are significantly more radiogenic than the shergottites (e.g., Foley et al., 2005), demonstrating that they are derived from a fundamentally different mantle source region than the shergottites.

Geochemical modeling of the shergottite source regions suggests that they could have formed as a result of solidification of a martian magma ocean (Borg et al., 1997; 2003; Borg and Draper, 2003; Elkins-Tanton, 2003), although formation through interaction of mantle and crustal reservoirs has also been proposed (Borg et al., 1997; Herd et al., 2002). Thus, isotopic mixing arrays defined by these samples are expected to record the age of large-scale silicate

differentiation on Mars (Shih et al., 1982) associated with primordial differentiation of the planet. The age of this silicate differentiation event is best determined using the ^{146}Sm – ^{142}Nd system of the shergottites due to the relatively short half-life of ^{146}Sm and the fact that Sm and Nd are both refractory lithophile elements. Ages derived from the ^{146}Sm – ^{142}Nd system are based on one of two assumptions. The most precise ages are three-stage Nd evolution model ages for individual samples that assume $^{147}\text{Sm}/^{144}\text{Nd}$ and $^{142}\text{Nd}/^{144}\text{Nd}$ values for bulk Mars (Harper et al., 1995; Borg et al., 1997; Debaille et al., 2007). The $^{142}\text{Nd}/^{144}\text{Nd}$ value for bulk Mars was originally assumed to be represented by terrestrial rocks, but most recently has been assumed to be the average value measured for chondritic meteorites. Ages for individual samples are strongly dependent on the assumed $^{142}\text{Nd}/^{144}\text{Nd}$ ratio of bulk Mars, however and vary by ~50 Ma depending on whether chondritic or terrestrial values are used in the calculation. This led to the development of whole rock isochron age determinations of martian differentiation based on the range of Sm–Nd isotopic compositions displayed by the shergottite meteorite suite (Borg et al., 2003; Foley et al., 2005; Caro et al., 2008). These ages are predicated on the hypothesis that the isotopic variability of the martian meteorite suite reflects mixing between complementary, contemporaneously-formed, isotopic reservoirs (Shih et al., 1982). However, previous ages determined using this approach are more imprecise than ages determined on individual samples. This is a reflection of the fact that uncertainty associated with ages defined by a suite of samples includes contributions from both analytical measurement and from scatter exhibited by the sample suite, whereas ages defined by single samples incorporate uncertainty associated only with individual measurements. The most accurate previous estimate of silicate differentiation is probably represented by the average of the published ages reported by (Borg et al., 1997; 2003; Foley et al., 2005; Debaille et al., 2007; Caro et al., 2008) which is 4530 ± 27 Ma (uncertainty defined by 2 standard deviations).

Tungsten isotopic measurements completed on the martian meteorites have been used to calculate model ages for Hf/W fractionation that was presumably associated with core formation on Mars. These models are strongly dependent on the assumed Hf/W ratio for bulk Mars. Furthermore, mechanisms to account for the difference between the ^{182}W isotopic compositions of shergottites and nakhlites are not well understood leading Halliday and Kleine (2006) to suggest that the silicate reservoirs on Mars are poorly mixed and to warn that caution should be used when applying W isotopic models to martian meteorites. Nevertheless, evidence for fractionation of Hf from W in martian meteorites is irrefutable and this system still provides the best constraint for the timing of martian core formation. Numerous ages of core formation have been calculated based on a range of model parameters. The most conservative estimate of the age of martian core formation is probably the average of these ages which is 4559 ± 8 Ma (average ± 2 standard deviations of ages reported by Kleine et al., 2004; 2009; Foley et al., 2005; Halliday and Kleine, 2006; Nimmo and Kleine, 2007; Dauphas and Pourmand, 2011). This calculated Hf–W age of core formation is within uncertainty of the average Sm–Nd age of silicate differentiation of 4530 ± 27 Ma inferred from the shergottites indicating that the duration of martian differentiation could have been as short as 10 Ma or as long as 64 Ma after formation of the first solar system solids. A short time interval between core formation and silicate differentiation would imply the martian core and mantle formed more or less simultaneously,

whereas a long time interval would imply that the planet had a protracted accretion and differentiation history. In order to more accurately define the duration of planetary accretion and differentiation on Mars, we have completed high-precision Sm–Nd isotopic measurements on a suite of martian shergottites and used these as a basis to rigorously evaluate and further develop various approaches to constrain the differentiation age of the shergottite source regions.

2. METHODS

High precision $^{147}\text{Sm}/^{144}\text{Nd}$ – $^{143}\text{Nd}/^{144}\text{Nd}$ – $^{142}\text{Nd}/^{144}\text{Nd}$ and $^{87}\text{Rb}/^{86}\text{Sr}$ – $^{87}\text{Sr}/^{86}\text{Sr}$ isotopic measurements have been completed on 10 basaltic martian meteorites exhibiting trace element characteristics indicative of derivation from the observed range of enriched and depleted source regions. An additional relatively small aliquot of the depleted shergottite Dhofar 019 has been analyzed for $^{147}\text{Sm}/^{144}\text{Nd}$ – $^{143}\text{Nd}/^{144}\text{Nd}$ and $^{87}\text{Rb}/^{86}\text{Sr}$ – $^{87}\text{Sr}/^{86}\text{Sr}$ as well. The high precision measurements were completed on 5 meteorites with Sr and Nd isotopic systematics of an enriched source region (Los Angeles, NWA1068, Dho378, NWA4468, and NWA4878), 3 with Sr and Nd isotopic systematics of a depleted source region (Tissint, DaG476, and SaU005) and 2 of intermediate composition (EET79001A and NWA480). Large fractions of these samples were dissolved after washing in water and 0.1M acetic acid in a Class 100 laboratory at Lawrence Livermore National Laboratory (LLNL). Small fractions were spiked using mixed ^{149}Sm – ^{150}Nd tracer and ^{87}Rb – ^{84}Sr tracers to obtain whole rock $^{147}\text{Sm}/^{144}\text{Nd}$ and $^{87}\text{Rb}/^{86}\text{Sr}$ values. These concentration data are presented in Table 1.

Both spiked and unspiked samples were purified using a combination of ion-exchange chromatographic procedures. Rubidium, strontium, and rare earth elements (REE) were purified using 2N HCl, 2N HNO₃, and 6N HCl acids and AG 50W-X8 200-400 mesh resin in quartz columns. Strontium was further purified using Sr-Spec resin in 100 μL Teflon columns with 1 N HNO₃ and H₂O. The Sm and Nd were separated in pressurized quartz columns using 0.2M alpha-hydroxyisobutyric acid buffered to pH = 4.4 and AG 50W-X8 200-400 mesh resin converted to NH₄ form. Unspiked Nd fractions analyzed for $^{142}\text{Nd}/^{144}\text{Nd}$ ratios were put through this procedure twice to remove Ce. Total procedural blanks including digestions were Rb = 9 pg, Sr = 21 pg, Sm = 8 pg and Nd = 22 pg.

Isotopic analyses were obtained using a ThermoScientific Triton thermal ionization mass spectrometer at LLNL. Neodymium and samarium were loaded in 2N HCl onto zone refined Re double filaments. High precision $^{142}\text{Nd}/^{144}\text{Nd}$ ratios were obtained through multi-dynamic analyses at high intensity (up to 4.9×10^{-11} amperes ^{144}Nd) and long duration (up to 13.5 hours) on the unspiked Nd fractions. Neodymium was corrected for instrumental mass fractionation using $^{146}\text{Nd}/^{144}\text{Nd} = 0.7219$. Isobaric interferences on Nd were monitored using ^{140}Ce and ^{149}Sm . Cerium corrections ranged from 0 to 36 ppm, whereas Sm interference corrections were less than 2 ppm. Average values determined on Nd and Sm isotopic standards are presented in Table 2. Replicate $^{142}\text{Nd}/^{144}\text{Nd}$ analyses completed on martian meteorites and terrestrial standards during the course of this investigation agreed within 3 ppm. The maximum difference between four

samples analyzed by both Debaille et al. (2007) and in this investigation was also 3 ppm. Neodymium isotope dilution measurements were completed using static acquisition in which 200 eight-second integrations were collected. The isotopic composition of Sm was obtained from unspiked fractions of the meteorites using a static acquisition routine consisting of 200 eight-second integrations. The intensity of these runs were 1.0 to 1.8×10^{-11} amperes ^{149}Sm . Samarium concentrations were determined using the same routine on the spiked fractions. Samarium was corrected for mass fractionation assuming $^{147}\text{Sm}/^{152}\text{Sm} = 0.56081$. Isobaric interferences for Sm were monitored using ^{155}Gd and ^{146}Nd and were less than 2 ppm. The Sm isotopic data obtained during this investigation is presented in Table 3.

Rubidium was loaded on single zone refined Re filaments in 2N HCl with a 99.999% pure Ta_2O_5 emitter suspended in 0.5M H_3PO_4 . Fractionation was corrected using runs of NBS-984 completed during the course of the investigation. Strontium was also loaded on single zone refined Re filaments in 2N HCl with the Ta_2O_5 emitter and run at 3 to 6×10^{-11} amps ^{88}Sr for 200 ratios of 16 second integrations. Fractionation was corrected assuming $^{86}\text{Sr}/^{88}\text{Sr} = 0.1194$. Although ^{85}Rb was monitored during the analyses, it was not detected during Sr measurements. Strontium isotopic compositions of samples and standards completed during the course of this investigation are presented in Table 2.

3. RESULTS

3.1. Samarium isotopic compositions

The Sm isotopic composition of the shergottites was determined in order to assess if they have been modified by the capture of thermal neutrons on the martian surface (Table 3). This phenomenon is well known on the Moon where galactic cosmic rays produce thermal neutrons that are captured by isotopes, such as ^{149}Sm , that have exceedingly large neutron capture cross sections (Russ, 1972). Such modification of the ^{149}Sm abundance of a sample will affect the $^{147}\text{Sm}/^{144}\text{Nd}$ ratio if undetected. An excessively large thermal neutron fluence, such as is observed on the Moon, can even affect the $^{142}\text{Nd}/^{144}\text{Nd}$ ratios of the samples (Nyquist et al., 1995). Our data indicate, however, that the Sm isotopic compositions of the shergottites are within analytical uncertainty of values obtained on terrestrial rock and isotopic standards. The slight excesses reported in ^{150}Sm determined for Los Angeles and Tissint are most likely caused by isobaric interferences from ^{150}Nd in these samples ($^{146}\text{Nd}/^{152}\text{Sm}$ up to 0.0016) because these samples demonstrate no evidence for corresponding deficits in ^{149}Sm . Thus, the ^{149}Sm data suggest that levels of thermal neutron radiation have been low near the martian surface over the past ~600 Ma so that $^{147}\text{Sm}/^{144}\text{Nd}$ and $^{142}\text{Nd}/^{144}\text{Nd}$ ratios determined on the shergottites require no corrections.

3.2 Neodymium and strontium isotopic compositions

Isotope dilution $^{87}\text{Rb}/^{86}\text{Sr}$ and $^{147}\text{Sm}/^{144}\text{Nd}$ determined on the shergottites are presented in Table 1, whereas $^{87}\text{Sr}/^{86}\text{Sr}$, $^{143}\text{Nd}/^{144}\text{Nd}$, and $^{142}\text{Nd}/^{144}\text{Nd}$ are presented in Table 2. The isotopic compositions of terrestrial rock and mass spectrometry standards are also presented in Table 2. In general, the shergottite data is similar to that previously reported for similar martian meteorites (see summary in Nyquist et al., 2001). The $^{87}\text{Rb}/^{86}\text{Sr}$ ratios determined for the suite of meteorites is highly variable ranging from 0.006 to 0.35. Although the range of $^{87}\text{Rb}/^{86}\text{Sr}$ generally correlates with shergottite subgroup (depleted, intermediate, enriched) there is some overlap. The $^{147}\text{Sm}/^{144}\text{Nd}$ ratios measured for this suite of shergottites is typical (Debaille et al., 2007; Caro et al., 2008) ranging from 0.23 to 0.51 and mostly correlating with shergottite subgroup. The depleted subgroup, however, demonstrates a large range of $^{147}\text{Sm}/^{144}\text{Nd}$ ratios from 0.38 to 0.51 overlapping the range defined by the intermediate group. The Sr and Nd isotopic compositions correlate well with the shergottite subgroup. The depleted shergottites have $^{87}\text{Sr}/^{86}\text{Sr} = 0.701\text{--}0.708$, $^{143}\text{Nd}/^{144}\text{Nd} = 0.5151\text{--}0.5155$, and $^{142}\text{Nd}/^{144}\text{Nd} = 1.141911\text{--}1.141920$ ($\epsilon^{142}\text{Nd} = +0.57$ to $+0.72$). The intermediate shergottites have $^{87}\text{Sr}/^{86}\text{Sr} = 0.710\text{--}0.713$, $^{143}\text{Nd}/^{144}\text{Nd} = 0.5134\text{--}0.5137$, and $^{142}\text{Nd}/^{144}\text{Nd} = 1.141854\text{--}1.141863$ ($\epsilon^{142}\text{Nd} = +0.15$ to $+0.23$). The isotopic composition of the enriched shergottites are remarkably consistent with $^{87}\text{Sr}/^{86}\text{Sr} = 0.718\text{--}0.723$, $^{143}\text{Nd}/^{144}\text{Nd} = 0.51231\text{--}0.51235$, and $^{142}\text{Nd}/^{144}\text{Nd} = 1.141813\text{--}1.141819$ ($\epsilon^{142}\text{Nd} = -0.21$ to -0.21). The Rb–Sr isotopic systematics of the shergottites analyzed in this study are quite variable reflecting both compositional differences inherited from their source regions and addition of terrestrial Sr during weathering in the desert localities where many of these samples were found. The desert meteorites display Sm–Nd isotopic systematics that are essentially identical to those determined from non-desert meteorites indicating that the Sm–Nd isotopic system has not been affected by weathering.

4. MODEL AGE CALCULATIONS

4.2. Samarium–neodymium ages

4.2.1 $^{147}\text{Sm}/^{144}\text{Nd}$ of basalt source regions

The Sm–Nd isotopic system provides a powerful tool with which to constrain the timing of silicate differentiation. This stems from the fact that it is comprised of two decay chains. The first is $^{147}\text{Sm} \rightarrow ^{143}\text{Nd}$ with a half-life of 106 Ga. This decay chain provides a record of the cumulate, long-term Sm/Nd elemental fractionation that occurred over the entire history of the planet beginning at 4567 Ma until the present. This system is therefore ideal to estimate the

average $^{147}\text{Sm}/^{144}\text{Nd}$ ratio of individual meteorite source regions. The second decay chain is $^{146}\text{Sm} \rightarrow ^{142}\text{Nd}$. Although the half-life for this system was recently determined to be 68 Ma (Kinoshita et al., 2012), the traditional half-life of 103 Ma appears to best reproduce the absolute ages of most planetary samples (Borg et al., 2014; Marks et al., in revision). Therefore, the 103 Ma half-life is used in the calculations presented here. The relatively short half-life of ^{146}Sm allows this decay chain to record the timing of geologic processes that fractionated Sm from Nd in the earliest stages of planetary history. When both Sm–Nd decay chains are used together in an iterative fashion, they can define the $^{147}\text{Sm}/^{144}\text{Nd}$, $^{143}\text{Nd}/^{144}\text{Nd}$, and $^{142}\text{Nd}/^{144}\text{Nd}$ ratios of planetary-scale source regions and the age of differentiation of these sources.

There are three types of Sm–Nd model age calculations that can be applied to determine the age of shergottite source region formation using the measured Sm–Nd isotopic compositions of bulk samples. These model age calculations are discussed separately below in the following sections. All three approaches used to determine the age of martian planetary differentiation require the present-day $^{147}\text{Sm}/^{144}\text{Nd}$ ratio of the shergottite source regions to be known. This can be estimated in two ways. In the first, the $^{147}\text{Sm}/^{144}\text{Nd}$ of the bulk rock is used as a proxy for the $^{147}\text{Sm}/^{144}\text{Nd}$ of the source region. This assumes that Sm is minimally fractionated from Nd during the partial melting event that produced the basaltic parental melts and that the accumulation of mineral phases in the basalts has not changed their Sm/Nd ratios. It has been demonstrated, however, that these assumptions may not be valid for Mars (Borg et al., 1997; 2003; Debaille et al., 2007). The $^{147}\text{Sm}/^{144}\text{Nd}$ ratios of the shergottites indicate that they are derived from more depleted source regions than is suggested by their $^{143}\text{Nd}/^{144}\text{Nd}$ ratios. For example, the $^{147}\text{Sm}/^{144}\text{Nd}$ ratios of the enriched subgroup shergottites are significantly higher (0.23–0.25) than the chondritic value of 0.1967, yet the meteorites have initial $\epsilon^{143}\text{Nd}$ values that range from -6 to -8 (Tables 1–2). Estimating the $^{147}\text{Sm}/^{144}\text{Nd}$ of the shergottite source region from the bulk rock $^{147}\text{Sm}/^{144}\text{Nd}$ values is therefore unlikely to be accurate.

The second way to calculate the $^{147}\text{Sm}/^{144}\text{Nd}$ ratio of basalt sources is presented in Equation 1 (Nyquist et al., 1995). The equation uses the age, as well as the $^{147}\text{Sm}/^{144}\text{Nd}$ and $^{143}\text{Nd}/^{144}\text{Nd}$ ratios of the basalts, and assumes that the Nd isotopic systematics reflect growth in three stages of evolution. The first stage of growth occurs in an undifferentiated reservoir that is assumed to have present-day $^{147}\text{Sm}/^{144}\text{Nd} = 0.1967$ and $^{143}\text{Nd}/^{144}\text{Nd} = 0.512638$ (Jacobsen and Wasserburg, 1980). The second stage occurs in the differentiated reservoir that formed at T_1 (calculated below to be 4504 Ma) until the age of eruption (i.e., crystallization) of the samples. The final stage occurs in the rock itself until the present time. Table 4 presents a summary of variables used in the following equations.

(Eq. 1)

$$\left(\frac{^{147}\text{Sm}}{^{144}\text{Nd}}\right)^S = \frac{\left[\left(\frac{^{143}\text{Nd}}{^{144}\text{Nd}}\right)^{M3} - \left(\frac{^{143}\text{Nd}}{^{144}\text{Nd}}\right)^{SSI} - \left(\frac{^{147}\text{Sm}}{^{144}\text{Nd}}\right)^{Ch} (e^{\lambda^{147}T_0} - e^{\lambda^{147}T_1}) - \left(\frac{^{147}\text{Sm}}{^{144}\text{Nd}}\right)^{M1} (e^{\lambda^{147}T_2} - 1)\right]}{(e^{\lambda^{147}T_1} - e^{\lambda^{147}T_2})}$$

The approach used to calculate the $^{147}\text{Sm}/^{144}\text{Nd}$ ratio of the meteorite source regions is consistent with the three-stage model age calculations presented below to determine the age of source differentiation because both sets of equations assume growth in identical reservoirs. The $^{147}\text{Sm}/^{144}\text{Nd}$ of the source, however, is also dependent on the age of differentiation. Thus, the $^{147}\text{Sm}/^{144}\text{Nd}$ of the source and the age of the source must be derived simultaneously (see equations 2, 3, 4i, and 4j below).

4.2.2. $^{142}\text{Nd}/^{144}\text{Nd}$ of bulk Mars

In order to obtain $^{146}\text{Sm}-^{142}\text{Nd}$ model ages of differentiation from Sm–Nd measurements completed on individual samples the $^{147}\text{Sm}/^{144}\text{Nd}$ and $^{142}\text{Nd}/^{144}\text{Nd}$ of bulk Mars must be known. Previous ages of martian silicate differentiation have been calculated assuming either terrestrial or chondritic $^{142}\text{Nd}/^{144}\text{Nd}$ ratios (Harper et al., 1995; Borg et al., 1997; Debaille et al., 2007). Whereas limited fractionation of Sm/Nd in geologic environments allows the $^{147}\text{Sm}/^{144}\text{Nd}$ of bulk planets to be fairly well constrained by the analysis of chondritic meteorites, the bulk $^{142}\text{Nd}/^{144}\text{Nd}$ ratio appears to be more variable in planetary materials (e.g., Boyet et al., 2005; Boyet and Carlson, 2010). The initial $^{142}\text{Nd}/^{144}\text{Nd}$ ratio of Mars can also be obtained from the Sm–Nd and Nd–Nd isochron diagrams presented in Figures 1 and 2. The initial $\epsilon^{142}\text{Nd}$ value derived from the y-intercept of Figure 1 is consistent with derivation of the martian source regions from an undifferentiated reservoir with a $^{147}\text{Sm}/^{144}\text{Nd}$ of 0.1967 and a present-day $^{142}\text{Nd}/^{144}\text{Nd}$ ratio of 1.141830 ± 7 ($\epsilon^{142}\text{Nd} = -0.06 \pm 0.06$). Figure 2 is an $\epsilon^{142}\text{Nd}-\epsilon^{143}\text{Nd}$ isochron plot, that provides an estimate of the present-day $^{142}\text{Nd}/^{144}\text{Nd}$ ratio that is independent of the present-day $^{142}\text{Nd}/^{144}\text{Nd}$ ratio defined by the intercept in Figure 1. Figure 2 yields a nearly identical present-day $\epsilon^{142}\text{Nd}$ value of bulk Mars of 1.141830 ± 2 ($\epsilon^{142}\text{Nd} = -0.06 \pm 0.02$). The present-day $^{142}\text{Nd}/^{144}\text{Nd}$ ratio estimated for Mars from the isochron plots is within uncertainty of the values measured in our laboratory on terrestrial Nd and whole rock standards (Table 1), suggesting that the Sm–Nd isotopic systematics of Mars and Earth are very similar. Both this $^{142}\text{Nd}/^{144}\text{Nd}$ value as well as the chondritic $^{142}\text{Nd}/^{144}\text{Nd}$ value are used in the following calculations.

4.2.3. Three stage model age for individual samples

The simplest approach to determine the age of differentiation of the shergottite source regions is to calculate three-stage model ages on single samples using Equations 1 and 2. Note

that Equation 2 is structurally identical to the equation used for other short-lived chronometers such as Hf–W model ages (e.g., Kleine et al., 2009). The advantage of the Sm–Nd system over other short-lived chronometers is that the ratio of parent/daughter elements (expressed in equation 2 as $\left(\frac{^{147}\text{Sm}}{^{144}\text{Nd}}\right)^S$) can be determined from $^{143}\text{Nd}/^{144}\text{Nd}$ isotopic measurements of the samples, rather than estimated from their bulk chemistry which is influenced by magma production (partial melting) and magma differentiation (crystallization and mineral accumulation) processes. Thus, the $^{147}\text{Sm}/^{144}\text{Nd}$ of the source used in this equation is calculated from Equation 1 assuming 3 stages of evolution. This age calculation is therefore considered to be a three-stage model age despite the fact that the third stage of $^{142}\text{Nd}/^{144}\text{Nd}$ growth in the rocks is ignored because of their young crystallization ages. Note that all ages calculated here are referenced to the age of CAIs of 4567 Ma (Amelin et al., 2002; Connelly et al., 2008)

(Eq. 2)

$$Age = 4567 - \left(\frac{1}{\lambda^{146}}\right) \ln \left\{ \left(\frac{^{146}\text{Sm}}{^{144}\text{Sm}}\right)^{SSI} \frac{\left(\frac{^{147}\text{Sm}}{^{144}\text{Nd}}\right)^S \left(\frac{^{144}\text{Sm}}{^{147}\text{Sm}}\right)^{Std} - \left(\frac{^{147}\text{Sm}}{^{144}\text{Nd}}\right)^{Ch} \left(\frac{^{144}\text{Sm}}{^{147}\text{Sm}}\right)^{Std}}{\left(\frac{^{142}\text{Nd}}{^{144}\text{Nd}}\right)^{M2} - \left(\frac{^{142}\text{Nd}}{^{144}\text{Nd}}\right)^B} \right\}$$

Model ages derived from Equation 2 are strongly dependent on the $^{142}\text{Nd}/^{144}\text{Nd}$ ratio that is assumed for the bulk planet prior to differentiation. If Mars is assumed to have a chondritic $^{142}\text{Nd}/^{144}\text{Nd}$ value, the measured Sm–Nd isotopic compositions of many of the shergottites do not permit Equations 1 and 2 to converge. The depleted and intermediate shergottites are the only subgroups for which the measured Nd isotopic compositions allow convergence. The average age of the depleted shergottites is 4531 ± 7 Ma, whereas the intermediate shergottites yield average ages that are older than the Solar System (4589 ± 50 Ma). The variation in the three-stage model ages for the depleted and intermediate shergottites, combined with the lack of convergence demonstrated by the Nd isotopic systematics of the enriched shergottites, implies that the assumption that shergottites evolved in three stages of evolution from a planet with a present-day bulk $^{142}\text{Nd}/^{144}\text{Nd}$ ratio of chondritic meteorites is not correct. However, if the $^{142}\text{Nd}/^{144}\text{Nd}$ of the bulk planet is assumed to be 1.141830, as derived from the y-intercepts on Figures 1 and 2 instead of the chondritic value, then the equations converge for all three subgroups of shergottites and yield an average age of 4504 ± 42 Ma (Table 2).

In contrast to the $^{142}\text{Nd}/^{144}\text{Nd}$ ratio of bulk Mars used in the three stage model age calculations for individual samples, the model age is not strongly dependent on the assumed $^{147}\text{Sm}/^{144}\text{Nd}$ ratio of the source used in the calculations. For example, a rise in the $^{147}\text{Sm}/^{144}\text{Nd}$ ratio by 1% changes the average age of the shergottites less than 10 Ma. Similar shifts in age are obtained by changing the $^{142}\text{Nd}/^{144}\text{Nd}$ ratio assumed for the bulk planet by only 2 ppm. Thus, the

largest source of uncertainty in ages obtained from single samples is the assumed bulk $^{142}\text{Nd}/^{144}\text{Nd}$ ratio of Mars. The strong dependence of three-stage model ages determined for individual meteorites on the assumed $^{142}\text{Nd}/^{144}\text{Nd}$ ratio of the bulk planet, combined with observations that suggest the chondritic ratio may be a poor proxy for other planetary bodies (Borg et al., 2011, 2013, 2014; Marks et al., in revision) underscores the main weakness of using this approach to calculate differentiation ages.

4.2.4. Whole rock $^{146}\text{Sm}-^{142}\text{Nd}$ isochron age

The second approach used to determine the age of martian source differentiation is based on $^{146}\text{Sm}-^{142}\text{Nd}$ whole rock isochrons constructed using the $^{147}\text{Sm}/^{144}\text{Nd}$ ratios of the source regions, calculated for each meteorite using Equation 1, and the $^{142}\text{Nd}/^{144}\text{Nd}$ ratio measured in the bulk meteorite samples (Nyquist et al. 1995; Rankenburg et al., 2006; Boyet and Carlson, 2007; Caro et al., 2008; Brandon et al., 2009). The justification for constraining martian differentiation using the whole rock $^{146}\text{Sm}-^{142}\text{Nd}$ or whole rock $^{142}\text{Nd}/^{144}\text{Nd}-^{143}\text{Nd}/^{144}\text{Nd}$ isochron methods is the observation that the calculated isotopic compositions of the shergottite sources fall on binary mixing arrays with end-members that are compositionally similar to magma ocean source regions present on the Moon (Borg et al., 2003), as well as compositions modeled for martian magma ocean cumulates (Borg and Draper, 2003; Elkins-Tanton, 2003). Thus, the geochemical characteristics of the martian meteorite sources are consistent with derivation from a common reservoir at the same time. The variation in the isotopic composition of these sources is therefore likely to record their age of formation.

Equation 3 is used to calculate ages from the slope of the $^{147}\text{Sm}/^{144}\text{Nd}-^{142}\text{Nd}/^{144}\text{Nd}$ isochron plot (Figure 1). Slopes are regressed through the data using IsoPlot 4.15. Like the three-stage model ages determined on individual samples, the $^{147}\text{Sm}/^{144}\text{Nd}$ ratio of the source is dependent on the age of differentiation. Thus, the age derived from the slope of the $^{146}\text{Sm}-^{142}\text{Nd}$ isochron (Eq. 3) must be solved iteratively with the $^{147}\text{Sm}/^{144}\text{Nd}$ ratio of the source (Eq. 1). The ^{147}Sm isotope is used to represent Sm concentrations on the x-axis of this plot instead of the traditional ^{144}Sm isotope because this ratio is calculated from the $^{143}\text{Nd}/^{144}\text{Nd}$ ratio (Eq. 1). As a consequence, the slope derived from the isochron presented in Figure 1 yields an initial $^{146}\text{Sm}/^{147}\text{Sm}$ ratio rather than a $^{146}\text{Sm}/^{144}\text{Sm}$ ratio. Therefore Equation 3 is formulated to yield an age from a slope in the form $^{146}\text{Sm}/^{147}\text{Sm}$. Note that the $^{147}\text{Sm}/^{144}\text{Sm}$ ratios of individual samples were measured and found to match the ratio determined on the AMES Sm standard (Table 3). Therefore this formulization yields results that identical to results based on the slope determined from a $^{144}\text{Sm}/^{144}\text{Nd}-^{142}\text{Nd}/^{144}\text{Nd}$ isochron plot. The age of differentiation (T_1) is expressed as:

$$(Eq. 3) \quad T_1 = 4567 - \left(\frac{1}{-\lambda^{146}} \right) \ln \left[\frac{m}{\left(\frac{^{146}\text{Sm}}{^{144}\text{Sm}} \right)^{SSI} \left(\frac{^{144}\text{Sm}}{^{147}\text{Sm}} \right)^{Std}} \right]$$

In this model, the ^{146}Sm – ^{142}Nd isochron is interpreted to represent a mixing line that has chronologic significance. Thus, the source regions of the shergottites appear to be derived from a common reservoir at the age defined by the ^{146}Sm – ^{142}Nd isochron. The model age of silicate differentiation determined from our data using this approach is 4504 ± 7 Ma. Unlike the three-stage model ages determined for individual samples using Equation 2, this age is not dependent on an assumed $^{142}\text{Nd}/^{144}\text{Nd}$ ratio for bulk Mars (Fig. 1). The age calculated using Equation 3 however, is slightly dependent on the $^{147}\text{Sm}/^{144}\text{Nd}$ ratio used to calculate the $^{143}\text{Nd}/^{144}\text{Nd}$ of the source regions from the initial $^{143}\text{Nd}/^{144}\text{Nd}$ values of the meteorites. For example, an age calculation in which the $^{147}\text{Sm}/^{144}\text{Nd}$ of the shergottite sources are arbitrarily shifted by 1% translates to a ~ 2 Ma shift in age. The ^{146}Sm – ^{142}Nd isochron has a mean squared weighted deviation (MSWD) of 2.2, indicating that the linear regression is a good fit to the data. A slightly more precise age is calculated if the Sm–Nd isotopic data obtained by Debaille et al. (2007) are included in this calculation. In this case, an age of 4504 ± 5 Ma is determined (MSWD = 2.0). This is our preferred age of silicate differentiation determined using this approach.

The initial $^{142}\text{Nd}/^{144}\text{Nd}$ determined from the ^{146}Sm – ^{142}Nd isochron is 1.1416154 ± 75 ($\epsilon^{142}\text{Nd}$ value = -1.941 ± 0.066). This corresponds to derivation of the martian source regions from an undifferentiated reservoir with present-day $^{147}\text{Sm}/^{144}\text{Nd}$ and $^{142}\text{Nd}/^{144}\text{Nd}$ ratio of 0.1967 and 1.141830, respectively, at 4504 Ma. The ^{146}Sm – ^{142}Nd isochron age is in excellent agreement with the average of the three-stage model ages determined on individual samples (4504 ± 42 Ma), which assumes that Mars had a bulk planet $^{142}\text{Nd}/^{144}\text{Nd}$ ratio of 1.141830. Thus, the ages and initial isotopic compositions derived from both the three-stage model for individual meteorites and the isochron age calculation derived from the entire suite of shergottites are consistent.

4.2.5. Whole rock $^{142}\text{Nd}/^{144}\text{Nd}$ and $^{143}\text{Nd}/^{144}\text{Nd}$ isochron age

The third approach used to constrain the age of differentiation of the shergottite source region uses the present-day $^{142}\text{Nd}/^{144}\text{Nd}$ and $^{143}\text{Nd}/^{144}\text{Nd}$ ratios of the shergottite sources and is presented in Figure 2. The $^{142}\text{Nd}/^{144}\text{Nd}$ of the source region today is the same as is measured for the shergottites, whereas the $^{143}\text{Nd}/^{144}\text{Nd}$ ratio of the source today is calculated from the initial $^{143}\text{Nd}/^{144}\text{Nd}$ ratio of the sample at the time of crystallization and the $^{147}\text{Sm}/^{144}\text{Nd}$ calculated for the source using Equation 1. This approach is based on the fact that the slope on a $^{142}\text{Nd}/^{144}\text{Nd}$ versus $^{143}\text{Nd}/^{144}\text{Nd}$ diagram (or $\epsilon^{142}\text{Nd}$ – $\epsilon^{143}\text{Nd}$ plot) corresponds to a three-stage model age (Borg et al., 2003; Foley et al., 2005). Whereas equations 1–3 are formulated by simply

rearranging simple decay equations or previously published equations (e.g., Nyquist et al. 1995; Caro et al., 2008; Kleine et al., 2009), equation 4 has not been derived previously. In fact, previous Nd–Nd ages reported in the literature appear to be derived using an iterative graphical approach (Borg et al., 2003; Foley et al., 2005). The derivation is therefore presented below.

This derivation is predicated upon expressing the slope of the $^{142}\text{Nd}/^{144}\text{Nd}$ versus $^{143}\text{Nd}/^{144}\text{Nd}$ plot in terms of T_1 , the age of the Sm/Nd fractionation. In the context of a whole rock isochron, T_1 is the time of differentiation of the source regions from a common reservoir. In the context of mineral fractions derived from a single sample, T_1 represents the age of crystallization of the sample. Like the previous expressions, the variables used in these equations are summarized in Table 4 except where specifically defined in the text.

The slope m is determined through regression analysis of the $^{142}\text{Nd}/^{144}\text{Nd}$ – $^{143}\text{Nd}/^{144}\text{Nd}$ isotope plot and is represented by:

$$(Eq. 4a) \quad m = \frac{\left(\frac{^{142}\text{Nd}}{^{144}\text{Nd}}\right)^{S1} - \left(\frac{^{142}\text{Nd}}{^{144}\text{Nd}}\right)^{S2}}{\left(\frac{^{143}\text{Nd}}{^{144}\text{Nd}}\right)^{S1} - \left(\frac{^{143}\text{Nd}}{^{144}\text{Nd}}\right)^{S2}}$$

where S1 and S2 refer to meteorite source regions with different, but arbitrary, $^{147}\text{Sm}/^{144}\text{Nd}$ ratios.

The denominator of equation 4a can be derived from equations expressing radiogenic growth in multiple reservoirs from an initial Solar System $^{143}\text{Nd}/^{144}\text{Nd}$ isotopic composition:

(e.q.4b)

$$\left(\frac{^{143}\text{Nd}}{^{144}\text{Nd}}\right)^{S1} = \left(\frac{^{143}\text{Nd}}{^{144}\text{Nd}}\right)^{SSI} + \left(\frac{^{147}\text{Sm}}{^{144}\text{Nd}}\right)^{Ch} (e^{\lambda^{147}T_0} - e^{\lambda^{147}T_1}) + \left(\frac{^{147}\text{Sm}}{^{144}\text{Nd}}\right)^{S1} (e^{\lambda^{147}T_1} - 1)$$

where $\left(\frac{^{147}\text{Sm}}{^{144}\text{Nd}}\right)^{S1}$ represents the composition of source 1. For a whole rock isochron $\left(\frac{^{143}\text{Nd}}{^{144}\text{Nd}}\right)^{SSI}$ represents the initial isotopic composition of the Solar System. For a mineral isochron this term represents the initial isotopic composition of the magma at the time of crystallization. Like many of the terms in this derivation, the value of this variable does not matter because it will be cancelled out in a later step.

A similar equation can be written for ^{143}Nd isotopic evolution in source 2. Subtracting the two equations and cancelling terms reduces the denominator of equation 4a to:

$$(Eq. 4c) \quad \left[\left(\frac{^{147}Sm}{^{144}Nd} \right)^{S1} - \left(\frac{^{147}Sm}{^{144}Nd} \right)^{S2} \right] (e^{\lambda^{147}T_1} - 1)$$

The numerator of equation 4a is derived in a similar fashion to equation 4b:

(Eq. 4d)

$$\begin{aligned} \left(\frac{^{142}Nd}{^{144}Nd} \right)^{S1} &= \left(\frac{^{142}Nd}{^{144}Nd} \right)^{SSI} + \left\{ \left(\frac{^{146}Sm}{^{144}Sm} \right)^{SSI} \left(\frac{^{144}Sm}{^{147}Sm} \right)^{Std} \left(\frac{^{147}Sm}{^{144}Nd} \right)^{Ch} [1 - e^{(-\lambda^{146}T_0) - (-\lambda^{146}T_1)}] \right\} \\ &+ \left\{ \left(\frac{^{146}Sm}{^{144}Sm} \right)^{SSI} [1 - e^{(-\lambda^{146}T_0) - (-\lambda^{146}T_1)}] \right\} \left(\frac{^{147}Sm}{^{144}Nd} \right)^{S1} \left(\frac{^{144}Sm}{^{147}Sm} \right)^{Std} [1 - e^{(-\lambda^{146}T_1)}] \end{aligned}$$

For a whole rock isochron $\left(\frac{^{142}Nd}{^{144}Nd} \right)^{SSI}$ represents the initial isotopic composition of the Solar System. For a mineral isochron this term represents the initial isotopic composition of the magma at the time of crystallization.

A similar equation can be written for ^{142}Nd isotopic evolution in source 2. Subtracting the two equations and cancelling terms reduces the numerator of equation 4a to:

$$(Eq. 4e) \quad \left[\left(\frac{^{147}Sm}{^{144}Nd} \right)^{S1} - \left(\frac{^{147}Sm}{^{144}Nd} \right)^{S2} \right] \left(\frac{^{146}Sm}{^{144}Sm} \right)^{SSI} \left(\frac{^{144}Sm}{^{147}Sm} \right)^{Std} [e^{(-\lambda^{146}T_0) - (-\lambda^{146}T_1)}]$$

Combining equations 4e and 4c into Equation 4a yields:

$$(Eq. 4f) \quad m = \frac{\left[\left(\frac{^{147}Sm}{^{144}Nd} \right)^{S1} - \left(\frac{^{147}Sm}{^{144}Nd} \right)^{S2} \right] \left(\frac{^{146}Sm}{^{144}Sm} \right)^{SSI} \left(\frac{^{144}Sm}{^{147}Sm} \right)^{Std} [e^{(-\lambda^{146}T_0) - (-\lambda^{146}T_1)}]}{\left[\left(\frac{^{147}Sm}{^{144}Nd} \right)^{S1} - \left(\frac{^{147}Sm}{^{144}Nd} \right)^{S2} \right] (e^{\lambda^{147}T_1} - 1)}$$

Rearranging equation 4f and canceling terms yields:

$$(Eq. 4g) \quad \left[(e^{\lambda^{147}T_1} - 1) \frac{m}{\left(\frac{^{146}Sm}{^{144}Sm}\right)^{SSI} \left(\frac{^{144}Sm}{^{147}Sm}\right)^{Std}} \right] = [e^{(-\lambda^{146}T_0)} - (-\lambda^{146}T_1)]$$

Taking the natural log yields:

$$(Eq. 4h) \quad \ln \left[(e^{\lambda^{147}T_1} - 1) \frac{m}{\left(\frac{^{146}Sm}{^{144}Sm}\right)^{SSI} \left(\frac{^{144}Sm}{^{147}Sm}\right)^{Std}} \right] = (-\lambda^{146}T_0) - (-\lambda^{146}T_1)$$

Rearranging equation 4h

$$(Eq. 4i) \quad T_1 = \left\{ (-\lambda^{146}T_0) - \ln \left[(e^{\lambda^{147}T_1} - 1) \frac{m}{\left(\frac{^{146}Sm}{^{144}Sm}\right)^{SSI} \left(\frac{^{144}Sm}{^{147}Sm}\right)^{Std}} \right] \right\} \left(\frac{1}{-\lambda^{146}} \right)$$

Note that T_1 is on both sides of the equation so that this equation must be solved iteratively. Solving the equation only takes a single iteration, however. Also note that the cancelation of terms in this derivation results in an age equation that is independent of any assumptions regarding the initial $^{142}Nd/^{144}Nd$ or $^{147}Sm/^{144}Nd$ composition of the bulk planet. As a result, this expression is also applicable to age determinations from mineral isochrons of any planetary sample demonstrating evidence for live ^{146}Sm . This is demonstrated in Table 5 in which ages calculated using equation 4i are compared to $^{147}Sm-^{143}Nd$ and $^{146}Sm-^{142}Nd$ mineral isochron ages we have recently published for lunar samples and an Allende CAI A13S4.

If the slope m is determined through regression on an $\varepsilon^{142}Nd-\varepsilon^{143}Nd$ plot instead of a $^{142}Nd/^{144}Nd-^{143}Nd/^{144}Nd$ plot the expression is easily modified to solve for T_1 by simply multiplying the slope by the ratio of values used to convert isotopic ratio measurements to epsilon notation.

$$(Eq. 4j) \quad T_1 = \left\{ (-\lambda^{146}T_0) - \ln \left[(e^{\lambda^{147}T_1} - 1) \frac{\left(\frac{{}^{142}\text{Nd}}{{}^{144}\text{Nd}}\right)^{Calc}}{\left(\frac{{}^{143}\text{Nd}}{{}^{144}\text{Nd}}\right)^{Calc(m)} \frac{\left(\frac{{}^{146}\text{Sm}}{\text{SSl}}\right)^{Std}}{\left(\frac{{}^{144}\text{Sm}}{\text{Std}}\right)^{Std}}} \right] \right\} \left(\frac{1}{-\lambda^{146}} \right)$$

Thus, for Nd measurements completed in our laboratory this ratio is expressed as:

$$(Eq. 4k) \quad \frac{\left(\frac{{}^{142}\text{Nd}}{{}^{144}\text{Nd}}\right)^{Calc}}{\left(\frac{{}^{143}\text{Nd}}{{}^{144}\text{Nd}}\right)^{Calc}} = \frac{1.141837}{0.512638}$$

The slope (m), defined by the regression on the $\epsilon^{142}\text{Nd}-\epsilon^{143}\text{Nd}$ plot (Fig. 2), is used in Equation 4j to calculate the age. The age is therefore completely independent of the ${}^{142}\text{Nd}/{}^{144}\text{Nd}$ assumed for bulk Mars and only weakly dependent on the calculated ${}^{147}\text{Sm}/{}^{144}\text{Nd}$ ratio of the meteorite sources. For example, a 1% change in ${}^{147}\text{Sm}/{}^{144}\text{Nd}$ ratio of a source translates into only a 0.5 Ma shift in age. This is therefore the preferred approach for calculating the differentiation age of the shergottite source regions. The slope determined from the combination of our data and the data of Debaille et al. (2007) is 0.01641 ± 52 (MSWD = 2.9), which corresponds to an age of 4504 ± 5 Ma. This age is in excellent agreement with the ages determined by the other techniques, but is more independent of assumptions regarding the Sm–Nd isotopic systematics of the meteorite source regions.

The initial ${}^{142}\text{Nd}/{}^{144}\text{Nd}$ of bulk Mars can be estimated from the y-intercept ($\epsilon^{143}\text{Nd} = 0$) on the $\epsilon^{142}\text{Nd}-\epsilon^{143}\text{Nd}$ isochron. The present-day initial ${}^{142}\text{Nd}/{}^{144}\text{Nd}$ value determined by the y-intercept is 1.141830 ± 0.000002 and is in excellent agreement with the present-day ${}^{142}\text{Nd}/{}^{144}\text{Nd}$ of 1.141830 ± 0.000008 derived from the ${}^{146}\text{Sm}-{}^{142}\text{Nd}$ isochron. The agreement between the ages and initial ${}^{142}\text{Nd}/{}^{144}\text{Nd}$ ratios calculated using all three models suggest that the shergottite source region formed at 4504 ± 5 Ma from a previously undifferentiated planet that has a present-day ${}^{147}\text{Sm}/{}^{144}\text{Nd}$ ratio of ~ 0.1967 and a ${}^{142}\text{Nd}/{}^{144}\text{Nd}$ ratio of ~ 1.141830 .

4.3. Rubidium-strontium model age calculation

The conclusion that Mars underwent planetary differentiation at ~ 4.5 Ga was originally proposed by Shih et al. (1982) on the basis of whole rock Rb–Sr systematics of the shergottites.

These authors noted that the bulk rock $^{87}\text{Rb}/^{86}\text{Sr}$ – $^{87}\text{Sr}/^{86}\text{Sr}$ compositions of the Shergotty, Zagami, and ALH77005 fell near a 4.5 Ga reference line that passed through the initial Sr isotopic composition of the Solar System derived from basaltic achondrites (BABI) by Papanastassiou and Wasserburg (1969). Shih et al. (1982) argued that the fact that the Rb–Sr systematics scattered around a ~4.5 Ga model isochron reflected the fact that the bulk rock $^{87}\text{Rb}/^{86}\text{Sr}$ ratios are a rough approximation of the ratios of the meteorite source regions.

Figure 3 is a plot of our bulk rock Rb–Sr isotopic compositions of the shergottites. The Rb–Sr data demonstrate significant scatter about a 4.50 Ga BABI reference line. The basaltic lithologies from non-desert environments fall closest to the reference line, whereas meteorites from desert environments generally fall to the left of the reference line. This reflects the fact that many of the meteorites found in desert environments have undergone terrestrial weathering that has resulted in the addition of terrestrial Sr. The presence of calcite in several of these samples (e.g., DaG 476) further supports this hypothesis (Zipfel et al., 2000). Note that not all meteorites found in desert environments lie to the left of the 4.50 Ga reference line indicating weathering has been relatively mild in some samples such as Dhofar 019, NWA 4468, and NWA 856. Likewise, not all non-desert meteorites line on the 4.50 Ga reference line. Deviation of these samples from the 4.50 Ga reference line indicates that the bulk rock $^{87}\text{Rb}/^{86}\text{Sr}$ ratio is not a perfectly faithful representation of the $^{87}\text{Rb}/^{86}\text{Sr}$ ratio of the source regions of the meteorites. Slight accumulation of plagioclase, for example with drive the ratio to the left in Figure 3 and accumulation of small amounts of trapped liquid will drive the whole rocks to the right. Despite these disturbances, the Rb–Sr isotopic systematics of the shergottites support the original hypothesis put forth by Shih et al. (1982) that the shergottite source regions formed at ~4.5 Ga and is consistent with the more precise age obtained from the Sm–Nd isotopic system.

5. DISCUSSION

5.1. Age of silicate differentiation

The age of 4504 ± 5 Ma calculated using Equation 4j is in good agreement with most of the previous age determinations for martian differentiation. These include 4525 ± 18 Ma (Borg et al., 1997), 4513^{+27}_{-33} Ma (Borg et al. 2003), 4525^{+19}_{-21} (Foley et al., 2005), and 4527 ± 18 Ma (Caro et al., 2008). The higher precision measurements obtained in this study from long-duration, high intensity multi-dynamic Nd analyses yield an age that is 4-6 times more precise however. Although the Sm–Nd isotopic data obtained in this study and by Debaille et al. (2007) are in excellent agreement, the ages calculated from the data differ outside analytical uncertainty. This reflects the fact that the age of 4535 ± 7 Ma calculated by Debaille et al. (2007) for three depleted shergottite source regions is a three-stage model age that assumes Mars had a chondritic $^{142}\text{Nd}/^{144}\text{Nd}$ isotopic composition (Equation 2). As noted above, model ages calculated for individual samples assuming a chondritic $^{142}\text{Nd}/^{144}\text{Nd}$ isotopic composition fail to converge for

all shergottites, suggesting that either the model calculation uses an incorrect parameter, or that the enriched and intermediate shergottites have had a more complex evolutionary history than the depleted shergottites.

Debaille et al. (2007) do in fact suggest that the enriched and intermediate shergottites contain a younger component that is absent from the depleted shergottites. The existence of the younger enriched reservoir is based on the observation that the $^{147}\text{Sm}/^{144}\text{Nd}$ ratios of the shergottites are higher than those calculated for their sources; a feature that is inconsistent with partial melting of olivine-pyroxene cumulates assumed to be representative of the shergottite sources. Debaille et al (2007) calculated the model age of the enriched source to be 4457 Ma from the $^{147}\text{Sm}/^{144}\text{Nd}$ and $^{142}\text{Nd}/^{144}\text{Nd}$ ratios inferred for this source. They defined the $^{147}\text{Sm}/^{144}\text{Nd}$ ratio of this enriched reservoir to be ≤ 0.159 from the intersection of a line regressed through the $^{147}\text{Sm}/^{144}\text{Nd}$ ratios measured for the bulk rocks versus $^{147}\text{Sm}/^{144}\text{Nd}$ ratios calculated for the meteorite sources and a 1:1 line on Figure 4. The present-day $^{142}\text{Nd}/^{144}\text{Nd}$ of the source was defined by the intersection of a line regressed through a plot of the shergottite Nd–Nd isotopic data and a Nd isotope growth curve modeled from a chondritic starting composition for a reservoir with a $^{147}\text{Sm}/^{144}\text{Nd}$ ratio of ≤ 0.159 . The age was calculated assuming bulk Mars had a chondritic Nd bulk isotopic composition.

Figure 4 is a reproduction of the $^{147}\text{Sm}/^{144}\text{Nd}$ whole rock versus $^{147}\text{Sm}/^{144}\text{Nd}$ source region plot that uses all currently available data. Whereas the older data were more or less linear, several newer data points for Tissint (Brennecka et al., 2014), Dhofar 019 (Caro et al., 2008; this study) and NWA 480 (this study) lie to the left of the line used to define the $^{147}\text{Sm}/^{144}\text{Nd}$ ratio of the enriched source by Debaille et al. (2007). The fact that meteorites derived from source regions with similar $^{147}\text{Sm}/^{144}\text{Nd}$ ratios have different $^{147}\text{Sm}/^{144}\text{Nd}$ ratios suggests the $^{147}\text{Sm}/^{144}\text{Nd}$ of the bulk rocks does not reflect binary mixing between enriched and depleted source regions. Instead, the $^{147}\text{Sm}/^{144}\text{Nd}$ ratios of the bulk rocks appear to be set relatively recently near the time the shergottite magmas were produced. The significance of the 4457 Ma age derived for a source with $^{147}\text{Sm}/^{144}\text{Nd}$ of 0.159 is therefore not clear.

5.2. Differentiation of Mars

Any petrogenetic model for martian differentiation must account for three observations: (1) a significant metal/silicate segregation event at 4559 ± 8 Ma, (2) a silicate differentiation of the shergottites source regions occurring at 4504 ± 5 Ma, and (3) preservation of differences in the ^{182}W isotopic composition of nakhlites and shergottites. If the Hf–W and Sm–Nd ages are interpreted to record core formation and silicate differentiation of Mars then there must be an extended period of 55 ± 13 Ma between core formation and silicate differentiation (Figure 5, Option 1). Debaille et al. (2007) also noted that the age of silicate differentiation inferred for their enriched reservoir was ~ 100 Ma younger than the age of core formation and argued that

magma ocean solidification was an extremely lengthy process due to the presence of a thick atmosphere on early Mars. Some thermal modeling initially supported this contention by suggesting that a shallow terrestrial magma ocean would cool in 100 Ma to 200 Ma in the presence of a thick atmosphere (e.g. Abe, 1997). However, more recent thermal modeling, incorporating constraints including complete compositional information, mineralogy, and internal dynamics of the Mars, by Elkins-Tanton (2008) demonstrates that mantle solidification occurred in less than 5 Ma even in the presence of a thick atmosphere. Thus, the discrepancy between Hf–W and Sm–Nd model ages is difficult to attribute to slow cooling of a magma ocean without an additional source of heat. Another potential difficulty associated with slow cooling of a magma ocean at 4504 Ma is that it does not account for the ^{182}W isotopic differences between the shergottites and nakhlites because ^{182}Hf would be extinct when the magma ocean was still at least partially liquid. A mechanism to prolong the duration of a magma ocean, or at least delay cooling a portion of the mantle, seems to be required.

If accretion occurred over an extended interval, then solidification of Mars could be delayed despite rapid heat flow from the planet as implied by thermal modeling (Figure 5; Option 2). Late accretion is expected to add heat into the system and could, in principle, help to maintain molten, undifferentiated, domains on the planet. If Mars is assumed to solidify in ~5 Ma after accretion ceased (Elkins-Tanton, 2008), then accretion must have lasted ~60 Ma in order to postpone differentiation of the shergottite mantle source regions until 4504 Ma. In this case, the metal/silicate segregation event recorded by the ^{182}Hf – ^{182}W isotopic system may reflect Hf/W fractionation that occurred both on planetesimals and during martian core formation. This scenario is appealing not only because it satisfies the thermal modeling, but also because it accounts for elevated abundances of highly siderophile elements (HSE) observed in the martian mantle. High abundances of these elements in terrestrial mantles are inconsistent with formation of metallic cores in closed geochemical systems because HSEs are strongly partitioned into the metal phase (e.g., Brandon et al., 2012). Accretion that occurred after core formation terminated could replenish the martian mantle in HSEs. Heterogeneous distribution of the later accreting material in the martian mantle might also explain the observed isotopic variation of ^{182}W in the different classes of martian meteorites.

A variation of this accretion scenario involves a late giant impact on Mars (Figure 5, Option 3). Such an impact has been suggested to be responsible for the formation of the northern lowlands of Mars (Wilheims and Squires, 1984; Andrews-Hanna et al., 2008; Marinova et al., 2008; Nimmo et al., 2008). Geophysical modeling of a martian giant impact event suggests that: (1) both Mars and the impactor are likely to be differentiated at the time of impact (Yoshino et al., 2003; Neumann et al., 2012), (2) the impact could heat a significant portion of the planet and induce melting (Tonks and Melosh, 1993; Monteux et al., 2007; Arkani-Hamed and Ghods, 2011), and (3) chemical global equilibrium between Mars and the impactor was probably not attained after the impact (Monteux and Arkani-Hamed, 2013). The Sm–Nd age could therefore record a differentiation event associated with cooling of a large, but not globally extensive, portion of the mantle after the impact. This hypothesis is consistent with the fact that the shergottites fall into a few young crystallization age groups (Nyquist et al., 2001; Borg and

Drake, 2005) and many have identical cosmic ray exposure ages (Nishiizumi et al., 2011) suggesting that they probably do not represent an extensive sampling of the martian surface. Several authors have suggested that the shergottites sample only a handful of sites on the martian surface (Nyquist et al., 2001; Borg and Drake, 2005; Brennecka et al., 2014). If this hypothesis is correct, then the age recorded in the Sm–Nd systematics of the shergottites might reflect a local, rather than a global, differentiation event. The Sm–Nd age would not define the age of martian silicate differentiation, but instead would place temporal constraints on the timing of the martian giant impact. Differences in ^{182}W isotopic compositions observed in martian meteorites could reflect heterogeneous distribution of W derived from Mars and the impactor in the martian mantle. This hypothesis implies that planet formation is a stochastic process in which accretion and differentiation occur contemporaneously over tens of millions of years, to produce numerous compositionally distinct geochemical reservoirs. If this scenario is correct, then neither ^{142}Nd nor ^{182}W constrain the timing of planetary scale differentiation events. The Sm–Nd age of 4504 ± 5 Ma only provides a minimum estimate for the age of martian planetary differentiation.

6. CONCLUSIONS

A mathematical expression to calculate an age from the slope defined by the regression on the $^{142}\text{Nd}/^{144}\text{Nd}$ – $^{143}\text{Nd}/^{144}\text{Nd}$ isochron is derived and used to calculate the age of shergottite source formation of 4504 ± 5 Ma from Sm–Nd isotopic data obtained on 11 martian meteorite samples. This age is in excellent agreement with ages calculated assuming three stage Nd evolution for individual samples, as well as with the age determined from a ^{146}Sm – ^{142}Nd whole rock isochron provided bulk Mars is assumed to have a near terrestrial $^{142}\text{Nd}/^{144}\text{Nd}$ value of 1.141830 ($\epsilon^{142}\text{Nd} = -0.06$). The Nd–Nd method is the preferred method to establish the age of the shergottite mantle source regions because it is independent of the assumed $^{142}\text{Nd}/^{144}\text{Nd}$ and $^{147}\text{Sm}/^{144}\text{Nd}$ ratio of bulk Mars. This age is in good agreement with most previous age determinations but is substantially more precise because Nd measurements were completed on long-duration high intensity multi-dynamic mass spectrometry runs. The young age of planetary differentiation requires that either solidification of the primordial martian magma ocean occurred over an extended period of 55 ± 13 Ma or that the Hf–W and/or Sm–Nd ages do not record planetary-scale differentiation events. Protracted cooling of the magma ocean is not consistent with some thermal models that suggest this process requires only a few million years to complete and does not account for the variability of ^{182}W isotopic compositions observed in the martian meteorites either. If the thermal modeling is correct, then an additional heat source appears to be required to keep the martian interior hot until 4504 Ma. Protracted accretion occurring more or less continuously for 60 Ma or a giant impact occurring around 4.5 Ga might provide such heat and could account for some of the isotopic compositions of the martian meteorites suite. Such an impact could produce a mantle that is compositionally heterogeneous on a planetary scale, as well as result in large scale melting of portions of the mantle relatively late in the history of

Mars. In this case, the 4504 ± 5 Ma Sm–Nd model age recorded in the shergottites could reflect differentiation associated the cooling of the mantle following a giant impact.

Acknowledgments

This work was performed under the auspices of the US Department of Energy by Lawrence Livermore National Laboratory under Contract DE-AC52-07NA27344. This document has been assigned release number LLNL-JRNL-XXXXX. The work was supported by National Aeronautics and Space Administration NASA Cosmochemistry grant NNH12AT84I (P.I. Borg).

References:

- Abe Y. (1997) Thermal and chemical evolution of the terrestrial magma ocean. *Phys. Earth Planet. Inter.* **100**, 27–39.
- Amelin Y., Krot A. N., Hutcheon I. D., Ulyanov A. A. (2002) Lead isotopic ages of chondrules and calcium-aluminum–rich inclusions. *Science* **296**, 1678-1683.
- Andrews-Hanna J. C., Zuber M. T., and Banerdt W. B. (2008) The Borealis basin and the origin of the martian crustal dichotomy. *Nature* **453**, 1212-1215.
- Arkani-Hamed J. and Ghods A. (2011) Could giant impact cripple core dynamos of small terrestrial planets? *Icarus* **212**, 920-934.
- Borg L. E. and Draper D. A. (2003) A petrogenetic model for the origin and compositional variation of the martian basaltic meteorites. *Meteor. Planet. Sci.* **38**, 1713-1731.
- Borg L. E. and Drake M. J. (2005) A Review of Meteorite Evidence for the Timing of Magmatism and of Surface or Near-Surface Liquid Water on Mars. *J. Geophys. Res.* **110**, E12SO3, doi:10.1029/2005JE002402.
- Borg L. E., Nyquist L. E., Wiesmann, H., Shih, C.-Y. (1997) Constraints on martian differentiation processes from Rb-Sr and Sm-Nd isotopic analyses of the basaltic shergottite QUE 94201. *Geochim. Cosmochim. Acta* **61**, 4915-4931.
- Borg L. E., Nyquist L. E., Reese Y., Wiesmann H., Shih C.-Y., Ivanova M., Nazarov M. A., and Taylor, L.A. (2001) The age of Dhofar 019 and its relationship to the other Martian meteorites *Lunar Planet. Sci.* **XXXIII** Abstr. #1144, CD-ROM.
- Borg L. E., Nyquist L. E., Wiesmann H., and Reese Y. (2002) Constraints on the petrogenesis of martian meteorites from Rb-Sr and Sm-Nd isotopic systematics of the lherzolithic shergottites ALH77005 and LEW88516. *Geochim. Cosmochim. Acta* **66**, 2037-2053.
- Borg L. E., Nyquist L. E., Wiesmann H., Reese Y. (2003) The age of Dar al Gani 476 and the differentiation history of the martian meteorites inferred from their Rb-Sr, Sm-Nd, and Lu-Hf isotopic systematics. *Geochim. Cosmochim. Acta* **67**, 3519-3536.

- Borg L. E., Edmunson J., Asmerom Y. (2005) Constraints on the U-Pb Isotopic Systematics of Mars Inferred from a Combined U-Pb, Rb-Sr, and Sm-Nd Isotopic Study of the Martian Meteorite Zagami. *Geochim. Cosmochim. Acta.* **69**, 5819-5830.
- Borg L. E., Connelly J. N., Boyet M., Carlson R. W. (2011) Evidence that the Moon is either young or did not have a global magma ocean. *Nature* **477**, 70-72.
- Borg L. E., Connelly J. N., Cassata W., Gaffney A. M., Carlson R. W., Papanastassiou D. A., Ramon E., Lindvall R., Bizarro M. (2013) Evidence for Widespread Magmatic Activity at 4.36 Ga in the Lunar Highlands from Young Ages Determined on Troctolite 76535. *Lunar Planet. Sci.* **XLIV** Abstr. #1563.
- Borg L. E., Brennecka G. A., Marks N., and Symes S. J. K. (2014) Neodymium Isotopic Evolution of the Solar System Inferred from Isochron Studies of Planetary Materials. *Lunar Planet. Sci.* **XLIV** Abstr. #1037
- Boyet M. and Carlson R.W. (2005) ^{142}Nd evidence for early (>4.53) global differentiation of the silicate Earth. *Science* **309**, 576-581.
- Boyet M. and Carlson, R. W. (2007) A highly depleted moon or a non-magma ocean origin for the lunar crust? *Earth Planet. Sci. Lett.* **263**, 505-516.
- Boyet M., Carlson R. W., and Horan M. (2010) Old Sm-Nd ages for cumulate eucrites and redetermination of the solar system initial $^{146}\text{Sm}/^{144}\text{Sm}$ ratio. *Earth Planet. Sci. Lett.* **291**, 172-181.
- Brandon A. D., Lapen T. L., Debaille V., Beard B. L., Rankenburg K., and Neal C. R. (2009) Re-evaluating $^{142}\text{Nd}/^{144}\text{Nd}$ in lunar mare basalts with implications for the early evolution and bulk Sm/Nd of the Moon. *Geochim. Cosmochim. Acta* **73**, 6421-6445.
- Brandon A. D., Puchtel I. S., Walker R. J., Day J. M. D., Irving, A. J., Taylor, L. A. (2012) Evolution of the martian mantle inferred from the ^{187}Re - ^{187}Os isotope and highly siderophile element abundance systematics of shergottite meteorites. *Geochim. Cosmochim. Acta.* **76**, 206-235.
- Brennecka G. A., Borg L. E., and Wadhwa M. (2014) Insights into the Martian Mantle: The Age and Isotopics of the Meteorite Fall Tissint. *Meteor. Planet. Sci.* **49**, 412-418.
- Carlson R. W., Borg L. E., Gaffney A. M., and Boyet M. (in press) Rb-Sr, Sm-Nd and Lu-Hf Isotope Systematics of the Lunar Mg-Suite: The Age of the Lunar Crust and its Relation to the Time of Moon Formation. *Proc. Roy. Soc. London.*
- Caro G., Bourdon B., Halliday A. N., and Quitte, G. (2008) Super-chondritic Sm/Nd ratios in Mars, the Earth and the Moon. *Nature* **452**, 336-339.
- Chambers J. E. (2004) Planetary accretion in the inner solar system. *Earth Planet. Sci. Lett.* **233**, 241-252
- Connelly J. N., Amelin Y., Krot A. N., and Bizzarro M. (2008). Chronology of the solar systems oldest solids. *Astrophys. J.* **675**, L121-L124.

- Dauphas N. and Pourmand A. (2011) Hf-W-Th evidence for rapid growth of Mars and its status as a planetary embryo. *Nature* **473**, 489-492.
- Debaille V., Brandon A. D., and Yin Q. -Z., Jacobsen, B. (2007) Coupled ^{142}Nd - ^{143}Nd evidence for a protracted magma ocean in Mars. *Nature* **450**, 525-528.
- Elkins-Tanton L. T. (2008) Linked magma ocean solidification and atmospheric growth for Earth and Mars. *Earth. Planet. Sci. Lett.* **271**, 181-191.
- Elkins-Tanton L. T., Parmentier E. M., and Hess P. C. (2003) Magma ocean fractional crystallization and cumulate overturn in terrestrial planets: implications for Mars. *Meteor. Planet. Sci.*, **38**, 1753–1771.
- Foley C. N., Wadhwa M., Borg L. E., Janney P. E., Hines R., and Grove T. L. (2005) The early differentiation history of Mars from ^{182}W - ^{142}Nd isotope systematics in the SNC meteorites. *Geochim. Cosmochim. Acta* **69**, 4557-4571.
- Halliday A. N., and Kleine, T. (2006) Meteorites and the timing, mechanisms, and conditions of terrestrial planet accretion and early differentiation. In *Meteorites and the early solar system II* (eds. D. S. Lauretta and H. Y. McSween Jr.) University of Arizona Press, pp. 775-801.
- Harper C. L., Nyquist L. E., Bansal B., Wiesmann H., and Shih, C. -Y. (1995) Rapid accretion and early differentiation of Mars indicated by $^{142}\text{Nd}/^{144}\text{Nd}$ in SNC meteorites. *Science* **267**, 213-217.
- Herd C. D. K., Borg L. E., Jones J. H., Papike J. J. (2002) Oxygen fugacity and geochemical variations in the martian basalts: Implications for martian basalt petrogenesis and the oxidation state of the upper mantle of Mars. *Geochim. Cosmochim. Acta* **66**, 2025-2036.
- Jacobsen S. B. and Wasserburg G. J. (1980) Sm-Nd isotopic evolution of chondrites. *Earth Planet. Sci. Lett.* **50**, 139-156.
- Kleine T., Touboul M., Bourdon B., Nimmo F., Mezger K., Palme H., Jaconsen S. B., Yin Q. – Z., Halliday A. N. (2009) Hf-W chronology of the accretion and early evolution of asteroids and terrestrial planets. *Geochim. et Cosmochim. Acta* **73**, 5150-5188.
- Kleine T., Mezger, K., Munker C., Palmer H., and Bischoff A. (2004) ^{182}Hf - ^{182}W isotope systematics of chondrites, eucrites and martian meteorites: Chronology of core formation and early mantle differentiation in Vesta and Mars. *Geochim. Cosmochim. Acta* **68**, 2935–2946.
- Kinoshita N., Paul M., Kashiv Y., Collon P., Deibel C. M., DiGiovine B., Greene J. P., Henderson D. J, Jiang C. L., Marley S. T., Nakanishi T, Pardo R. C., Rehm K. E., Roberston D, Scott R, Schmitt C, Tang X. D., Vondrasek R., and Yokoyama A. (2012) A Shorter ^{146}Sm Half-Life Measured and Implications for ^{146}Sm - ^{142}Nd Chronology in the Solar System. *Science* **335**, 1614-1617.
- Marks N. E., Borg L. E., Hutcheon I. D., Jacobsen B., Clayton R. N. (in revision) Samarium-neodymium chronology of an Allende calcium-aluminum-rich inclusion with implications for ^{146}Sm isotopic evolution. *Earth Planet. Sci. Lett.*

- Marks N. E., Borg L. E., Gaffney A. M. (2010) The Relationship of Northwest Africa 4468 to the Other Incompatible Element-enriched Shergottites Inferred from its Rb-Sr and Sm-Nd Isotopic Systematics. *Lunar Planet.Sci. XLI Houston TX*. abstract #2064.
- Marinova M. M., Aharonson O., and Asphaug E. (2008) Mega-impact formation of the Mars hemispheric dichotomy. *Nature*. **453**, 1216-1219.
- Monteux J., Coltice N., Dubuffet F., and Ricard Y. (2007) Thermo-mechanical adjustment after impacts during planetary growth. *Geophys. Res. Lett.* **34**, L24201.
- Monteux J. and Arkani-Hamed J. (2013) Consequences of giant impacts in early Mars: Core merging and Martian dynamo. *J. Geophys. Res. Planets*. **119**, doi 10.1002/2013JE004587.
- Neumann W. Breuer D., and Spohn T. (2012) Differentiation and core formation in accreting planetismals. *Astron. Astrophys.* **S43**, A141, 23.
- Nimmo F., Hart S. D., Korycansky D. G., and Agnor C. B. (2008) Implications of an impact origin for the Martian hemispheric dichotomy. *Nature* **453**, 120-1223.
- Nimmo F. and Kleine, T. (2007) How rapidly did Mars accrete? Uncertainties in the Hf-W timing or core formation. *Icarus* **191**, 497-504.
- Nishiizumi K., Nagao K., Caffee M. W., Jull A. J. T., and Irving A. J. (2011) Cosmic-ray exposure chronologies of depleted olivine-phyric shergottites. *Lunar. Planet. Sci. XLII* Abstract #2371.
- Nyquist L. E., Bogard D. D., Shih C. -Y., Greshake A., Stöffler D. and Eugster O. (2001) Ages and histories of martian meteorites. In *Chronology and Evolution of Mars* (eds. Kallenbach R., Geiss J. and Hartmann W. K.) Springer, pp. 105-164.
- Nyquist L.E., Wiesmann, H., Bansal, B.M., Shih, C.-Y., Keith, J.E., Harper, C.L. (1995) ^{146}Sm - ^{142}Nd formation interval for the lunar mantle. *Geochim. Cosmochim. Acta* **59**, 2817-2837.
- Nyquist L. E., Wooden J., Bansal B. M., Wiesmann H., McKay G., and Bogard D. D. (1979) Rb-Sr age of the Shergotty Achondrite and Implications for Metamorphic Resetting of Isochron Ages. *Geochim. Cosmochim. Acta* **43**, 1057-1074.
- Papanastassiou D. A. and Wasserburg G. J. (1969) Initial strontium isotopic abundances and the resolution of small time differences in the formation of planetary objects. *Earth Planet. Sci. Lett.* **5**, 361-376.
- Rankenburg K., Brandon A. D., and Neal C. R. (2006) Neodymium isotope evidence for a chondritic composition of the Moon. *Science* **312**, 1369-1372.
- Russ P. G., Burnett D. S., and Wasserburg, G. J. (1972) Lunar neutron stratigraphy. *Earth Planet. Sci. Lett.* **15**, 172-186.
- Shih C. -Y., Nyquist L. E., Bogard D. D., McKay G. A., Wooden J. L., Bansal B. M., Wiesmann H. (1982) Chronology and Petrogenesis of Young Achondrites, Shergotty, Zagami, and ALHA 77005: Late Magmatism on a Geologically Active Planet. *Geochim. Cosmochim. Acta* **46**, 2323-2344.

- Symes S. J. K., Borg L. E., Shearer C. K., and Irving A. J. (2008) The age of the martian meteorite Northwest Africa 1195 and the differentiation history of the shergottites. *Geochim. Cosmochim. Acta.* **72**, 1696-1710.
- Tonks W. B. and Melosh H. J. (1993) Magma ocean formation due to giant impacts. *J. Geophys. Res.* **98**, 5319-5333.
- Wilheims D. E. and Squires S. W. (1984) The Martian hemispheric dichotomy may be due to a giant impact. *Nature* **309**, 138-140.
- Yoshino T. Walter M. J., and Katsura T. (2003) Core formation in planetismals triggered by permeable flow. *Nature* **422**, 154-157.
- Zipfel J., Scherer P., Spettel B., Dreibus G, and Schultz L. (2000) Petrology and chemistry of the new shergottite Dar al Gani 476. *Meteor. Planet. Sci.* **35**, 95-106.

Table 1. Rb, Sr, Sm, and Nd concentration data

Sub-group	Sample	Weight (g)	Rb (ppm)	Sr (ppm)	$\left(\frac{^{87}\text{Rb}}{^{86}\text{Sr}}\right)^b$	Sm (ppm)	Nd (ppm)	$\left(\frac{^{147}\text{Sm}}{^{144}\text{Nd}}\right)^c$
Enriched	Los Angeles	0.231				2.161	5.576	0.23432 ± 23
	Dho 378	0.498	4.42	79.29	0.1612 ± 16	1.149	2.859	0.24301 ± 24
	NWA 856	0.207	5.19	41.99	0.3581 ± 36	0.9542	2.379	0.24247 ± 24
	NWA 4878	0.561	4.92	71.64	0.1989 ± 20	1.274	3.177	0.24245 ± 24
	NWA 1068	0.433	5.37	63.67	0.2441 ± 21	1.348	3.516	0.23182 ± 23
	NWA 4468	0.430				0.7559	1.917	0.23835 ± 24
	NWA 4468	0.394	3.06	26.39	0.3360 ± 33	0.5306	1.301	0.24650 ± 25
Inter-mediate	EET79001A	0.738	0.896	13.66	0.1898 ± 19	0.6183	0.892	0.41890 ± 42
	NWA 480	0.240	2.31	46.40	0.1440 ± 14	1.198	2.457	0.29478 ± 29
Depleted	DaG 476	1.812	0.531	57.95	0.02652 ± 27	0.3659	0.425	0.51689 ± 51
	SaU 005	1.839	0.298	79.30	0.01089 ± 11	0.4387	0.540	0.49071 ± 49
	Tissint	0.460	0.229	25.62	0.02590 ± 26	0.7159	1.116	0.38332 ± 38
	Dhofar 019 ^a	0.016	0.652	307.1	0.00615 ± 70	0.6698	1.079	0.37534 ± 38

^a Isotope dilution measurement only.

^b Error limits apply to last digits and include a minimum uncertainty of 1% plus 50% of the blank correction for Rb and Sr added quadratically.

^c Error limits apply to last digits and include a minimum uncertainty of 0.1% plus 50% of the blank correction for Sm and Nd added quadratically.

Table 2. Sm–Nd Isotopic Data

Sub-group	Sample	Age Sample (Ma) ^a	$\left(\frac{^{87}\text{Sr}}{^{86}\text{Sr}}\right)^d$	$\left(\frac{^{143}\text{Nd}}{^{144}\text{Nd}}\right)^e$	$\left(\frac{^{142}\text{Nd}}{^{144}\text{Nd}}\right)^e$	$\epsilon_{\text{Nd}}^{142}$	$\left(\frac{^{147}\text{Sm}}{^{144}\text{Nd}}\right)^f$	Model Age (Ma) ^g
Enriched	Los Angeles	170		0.512327 ± 1	1.141815 ± 3	-0.20	0.1844	4530 ± 23
	Dho 378	157	0.720922 ± 5	0.512335 ± 1	1.141813 ± 2	-0.21	0.1846	4549 ± 17
	NWA 856	170	0.723390 ± 7	0.512321 ± 2	1.141819 ± 6	-0.16	0.1839	4475 ± 61
	NWA 4878	170	0.720626 ± 6	0.512331 ± 1	1.141817 ± 2	-0.17	0.1842	4498 ± 24
	NWA 1068	185	0.717949 ± 5	0.512352 ± 1	1.141819 ± 2	-0.16	0.1852	4493 ± 23
	NWA 4468	187		0.512316 ± 1	1.141818 ± 4	-0.17	0.1837	4485 ± 39
	NWA 4468	187	0.720852 ± 5	0.512323 ± 1	1.141818 ± 3	-0.17	0.1836	4482 ± 27
Average (2SD)								4502 ± 55
Inter-mediate	EET79001A	173	0.712979 ± 5	0.513724 ± 2	1.141863 ± 7	+0.23	0.2257	4507 ± 36
	NWA 480	343	0.709702 ± 5	0.513380 ± 1	1.141854 ± 4	+0.15	0.2156	4522 ± 26
	Average (2SD)							
Depleted	DaG 476	474	0.707158 ± 6	0.515516 ± 1	1.141911 ± 4	+0.65	0.2670	4507 ± 8
	SaU 005	445	0.707034 ± 5	0.515324 ± 1	1.141902 ± 3	+0.57	0.2645	4495 ± 7
	Tissint	580	0.701039 ± 7	0.515506 ± 1	1.141920 ± 3	+0.72	0.2794	4498 ± 5
	Dhofar 019 ^c	574	0.707756 ± 9	0.515106 ± 25			0.2654	
	Ave, (2SD)							
Shergottite Average (2SD)								4504 ± 42
Terrestrial Standards	BCR-2		0.705000 ± 4	0.512621 ± 1	1.141831 ± 3	-0.05		
	BCR-2		0.705003 ± 4	0.512622 ± 1	1.141835 ± 3	-0.02		
	BCR-2		0.705003 ± 9					
	BHVO-2			0.512978 ± 2	1.141836 ± 3	-0.01		
	NBS-987 ^b		0.710249 ± 8					
	LaJolla ^b			0.511845 ± 8	1.141839 ± 6	+0.02		
	JNdi ^b			0.511201 ± 6	1.141837 ± 7	≅0.00		

^a Age of samples summarized in Nyquist et al. (2001), Borg and Drake (2005) and from Borg et al. (2001), Brennecka et al. (2014), and Marks et al. (2010).

^b Long-term average values obtained on standards. Uncertainties refer to last digits and are $2\sigma_p$ (2 x standard deviation of population of mass spectrometry runs on isotopic standard). NBS-987 standard average of N = 55 runs, BCR-2 standard average of N = 14 runs, JNdi standard average of N = 40 runs, LaJolla standard average of N = 12 runs.

^c Isotope dilution measurements only.

^d Measured value normalized to $^{86}\text{Sr}/^{88}\text{Sr} = 0.1194$. Uncertainties refer to last digits and are $2\sigma_m$ (2 x standard error of measured isotopic ratios)

^e Measured value normalized to $^{146}\text{Nd}/^{144}\text{Nd} = 0.7219$. Uncertainties refer to last digits and are $2\sigma_m$ (2 x standard error of measured isotopic ratios).

^f Value calculated from value equation 1.

^g Value calculated from equation 2 assuming bulk Mars has present-day $^{142}\text{Nd}/^{144}\text{Nd} = 1.141830$ (derived from the y-intercept in Figure 1A) and $^{147}\text{Sm}/^{144}\text{Nd} = 0.1967$. Uncertainties on individual model ages reflect the precision of the measured $^{142}\text{Nd}/^{144}\text{Nd}$ ratios, whereas the uncertainties on average model ages are $2\times$ the standard deviation of respective ages

Table 3. Samarium isotopic compositions

Sub-group	Sample	$\left(\frac{^{144}\text{Sm}}{^{152}\text{Sm}}\right)$	$\left(\frac{^{148}\text{Sm}}{^{152}\text{Sm}}\right)$	$\left(\frac{^{149}\text{Sm}}{^{152}\text{Sm}}\right)$	$\left(\frac{^{150}\text{Sm}}{^{152}\text{Sm}}\right)$	$\left(\frac{^{154}\text{Sm}}{^{152}\text{Sm}}\right)$	$\epsilon_{\text{Sm}}^{149}$	$\epsilon_{\text{Sm}}^{150}$
Enriched	Los Angeles	0.114977 ± 2	0.420437 ± 2	0.516847 ± 2	0.276002 ± 2	0.850797 ± 4	-0.08	+0.33
	NWA 856	0.114971 ± 3	0.420438 ± 3	0.516842 ± 3	0.275997 ± 2	0.850765 ± 5	-0.17	+0.14
	NWA 4878	0.114976 ± 2	0.420437 ± 2	0.516841 ± 2	0.275994 ± 2	0.850771 ± 6	-0.19	+0.04
	NWA 4468	0.114976 ± 2	0.420437 ± 3	0.516841 ± 3	0.275994 ± 2	0.850771 ± 5	-0.19	+0.04
Inter-mediate	EET79001A	0.114974 ± 2	0.420437 ± 2	0.516846 ± 3	0.275990 ± 2	0.850774 ± 5	-0.10	-0.11
	NWA 480	0.114971 ± 2	0.420436 ± 2	0.516848 ± 3	0.275991 ± 1	0.850766 ± 3	-0.06	-0.07
Depleted	DaG 476	0.114974 ± 2	0.420440 ± 3	0.516846 ± 3	0.275992 ± 2	0.850772 ± 5	-0.10	-0.04
	SaU 005	0.114973 ± 2	0.420437 ± 2	0.516849 ± 2	0.275991 ± 1	0.850775 ± 4	-0.04	-0.07
	Tissint	0.114953 ± 3	0.420447 ± 3	0.516850 ± 3	0.276001 ± 2	0.850762 ± 5	-0.02	+0.29
Terrestrial Standards	BCR-2	0.114975 ± 2	0.420438 ± 6	0.516851 ± 3	0.275992 ± 2	0.850795 ± 7	0.00	-0.03
	BCR-2	0.114977 ± 2	0.420440 ± 6	0.516854 ± 3	0.275994 ± 2	0.850793 ± 6	0.06	+0.04
	AMES ^a	0.114976 ± 7	0.420438 ± 8	0.516851 ± 8	0.275993 ± 3	0.850798 ± 9	≡0.00	≡0.00

Measured value normalized to $^{147}\text{Sm}/^{152}\text{Sm} = 0.56801$. Uncertainties refer to last digits and are $2\sigma_m$ ($2\times$ standard error of measured isotopic ratios).

^a Long-term average value obtained on AMES Sm standard (N=25). Uncertainties refer to last digits and are $2\sigma_p$ ($2\times$ standard deviation of population of mass spectrometry runs on isotopic standard).

Table 4. Variables used in equations 1-4

Variable	Description	Value
$(^{143}\text{Nd}/^{144}\text{Nd})^{\text{M3}}$	Present-day whole rock Nd isotopic ratio	Measured
$(^{142}\text{Nd}/^{144}\text{Nd})^{\text{M2}}$	Present-day whole rock Nd isotopic ratio	Measured
$(^{143}\text{Nd}/^{144}\text{Nd})^{\text{SSI}}$	Solar System initial Nd isotopic ratio	0.506674 ^a
$(^{142}\text{Nd}/^{144}\text{Nd})^{\text{B}}$	Bulk Mars Nd isotopic composition	1.141830
$(^{147}\text{Sm}/^{144}\text{Nd})^{\text{Ch}}$	Present-day bulk planet ratio (determined from analysis of chondritic meteorites)	0.1967 ^a
$(^{147}\text{Sm}/^{144}\text{Nd})^{\text{M1}}$	Present-day whole rock ratio	Measured
$(^{146}\text{Sm}/^{144}\text{Sm})^{\text{SSI}}$	Solar System initial Sm isotopic composition	0.00828 ^b
T_0	Age of Solar System (determined from CAIs)	4567 Ma ^c
T_1	Differentiation age of Mars	Solved for
T_2	Internal isochron age of martian meteorite	Measured
λ^{147}	^{147}Sm decay constant	$6.54 \times 10^{-6} \text{ Ma}^{-1}$
λ^{146}	^{146}Sm decay constant	$0.0067296 \text{ Ma}^{-1}$ ^b
$(^{144}\text{Sm}/^{147}\text{Sm})^{\text{Std}}$	Sm isotopic composition determined from terrestrial standards	0.202419
$(^{147}\text{Sm}/^{144}\text{Nd})^{\text{S}}$	Sm/Nd isotopic composition of shergottite source regions	Solved for
$(^{142}\text{Nd}/^{144}\text{Nd})^{\text{Calc}}$	Value used as denominator for calculating $\epsilon^{142}\text{Nd}$	1.141837
$(^{143}\text{Nd}/^{144}\text{Nd})^{\text{Calc}}$	Value used as denominator for calculating $\epsilon^{143}\text{Nd}$	0.512638

^a. Jacobsen and Wasserburg (1980)

^b. Marks et al. (in revision)

^c. Amelin et al. (2002); Connelly et al. (2008)

Table 5. Examples of Sm–Nd ages calculated using different methods

Sample	$^{147}\text{Sm}-^{143}\text{Nd}$ age (Ma)	$^{146}\text{Sm}-^{142}\text{Nd}$ age (Ma)	$^{142}\text{Nd}-^{143}\text{Nd}$ age (Ma)	Reference
60025	4367 ± 15	4318^{+30}_{-38}	4319^{+30}_{-38}	Borg et al. (2011)
76535	4307 ± 11	4300^{+29}_{-36}	4299^{+29}_{-36}	Borg et al. (2013)
60016	4300 ± 32	4298^{+57}_{-94}	4296^{+58}_{-97}	Marks et al. (2014)
77215	4283 ± 23	4348^{+59}_{-100}	4350^{+58}_{-96}	Carlson et al (in revision)
CAI A13S4 ^A	4560 ± 34	$4564^{+7.9}_{-8.4}$	$4565^{+8.0}_{-8.4}$	Marks et al. (in revision)

Ages calculated using $^{146}\text{Sm } t_{1/2} = 103 \text{ Ma}$ and $^{146}\text{Sm}/^{144}\text{Sm} = 0.00828$ following Marks et al. (in revision). CAI A13S4 age calculated using $^{146}\text{Sm}/^{144}\text{Sm} = 0.0084$ obtained from eucrite meteorites (Boyet et al., 2010). Slopes determined by regression of $^{143}\text{Nd}/^{144}\text{Nd}-^{142}\text{Nd}/^{144}\text{Nd}$ data are: 60025 = 0.0112 ± 0.0025 ; 76535 = 0.098 ± 0.0021 ; 60016 = 0.0096 ± 0.0046 ; 77215 = 0.0137 ± 0.0065 ; CAI A13S4 = 0.0561 ± 0.0031 .

Figure Captions

Figure 1. A ^{146}Sm – ^{142}Nd isochron plot used to determine the age of differentiation of the shergottite source regions. Data from this study are dark circles and data reported by Debaille et al. (2007) are open squares. The measured bulk meteorite $^{142}\text{Nd}/^{144}\text{Nd}$ versus the $^{147}\text{Sm}/^{144}\text{Nd}$ of martian meteorite source regions, calculated from the measured $^{143}\text{Nd}/^{144}\text{Nd}$ (Eq. 1). This isochron yields a $^{146}\text{Sm}/^{147}\text{Sm}$ slope of 0.001092 ± 35 (MSWD = 2.0) that corresponds to an age of 4504 ± 5 Ma (Eq. 3). This value is determined using the initial Solar System $^{146}\text{Sm}/^{144}\text{Sm}$ of 0.00828 ± 43 (Marks et al., in revision). The initial $^{142}\text{Nd}/^{144}\text{Nd}$ of this isochron is 1.1416154 ± 75 ($\epsilon^{142}\text{Nd} = -1.941 \pm 0.066$), which corresponds to a present-day $^{142}\text{Nd}/^{144}\text{Nd}$ of 1.141830, assuming bulk Mars has a $^{147}\text{Sm}/^{144}\text{Nd}$ similar to that of chondritic meteorites of 0.1967.

Figure 2. An $\epsilon^{142}\text{Nd}$ – $\epsilon^{143}\text{Nd}$ isochron plot used to determine the age of differentiation of the shergottite source regions. The measured bulk meteorite $\epsilon^{142}\text{Nd}$ value is plotted against the $\epsilon^{143}\text{Nd}$ value of the present-day source region calculated from the initial $^{143}\text{Nd}/^{144}\text{Nd}$ of the meteorite. An isochron regressed through the data (thick solid line) yields a slope of 0.01641 ± 52 (MSWD = 2.9), which corresponds to an age of 4504 ± 5 Ma (Eq. 4j). Vertical dashed lines are Nd isotopic growth curves calculated at different ages using $^{147}\text{Sm}/^{144}\text{Nd}$ of 0.17, 0.1967, 0.23, 0.26, and 0.29. Thin solid lines model isochrons are calculated at common ages using different $^{147}\text{Sm}/^{144}\text{Nd}$ ratios. From these isochrons are spaced at 50 Ma intervals starting at 4200 Ma, excluding 4500 Ma, but including 4567 Ma. The present-day initial $^{142}\text{Nd}/^{144}\text{Nd}$ value determined by the y-intercept is 1.141830 ± 2 and is in excellent agreement with the value from Figure 1. Note that unlike the three-stage model ages presented in Table 2 for individual meteorites, the isochron ages are not dependent on the assumed $^{142}\text{Nd}/^{144}\text{Nd}$ of bulk Mars. The similarity of the present-day martian $^{142}\text{Nd}/^{144}\text{Nd}$ values to bulk Earth (open star) suggests that the Nd isotopic composition of Mars and Earth are identical, within uncertainty. Chondritic Nd isotopic composition (solid star) is from Boyet and Carlson (2007).

Figure 3. A Rb–Sr isochron plot of shergottite whole rock data. Reference line has a slope corresponding to an age of 4.50 Ga and passes through Best Achondrite Basaltic Initial (BABI) $^{87}\text{Sr}/^{86}\text{Sr} = 0.69906$ (Papanastassiou and Wasserburg, 1969). Data from this study, Borg et al. (1997, 2001, 2002, 2003, 2005) Symes et al. (2008); Marks et al. (2010); Nyquist et al. (1979); Brennecka et al. (2014). Samples from desert environments generally fall to right of reference line as a result of terrestrial weathering and addition of Sr.

Figure 4. A plot of $^{147}\text{Sm}/^{144}\text{Nd}$ measured in the bulk meteorite versus the $^{147}\text{Sm}/^{144}\text{Nd}$ calculated for the source region from the bulk rock $^{143}\text{Nd}/^{144}\text{Nd}$ using Equation 1. Solid line to the right of the 1:1 line is from Debaille et al. (2007) and was used to define the $^{147}\text{Sm}/^{144}\text{Nd}$ ratio of 0.159 for their enriched shergottite source region. The data are from this study, Borg et al. (1997, 2002, 2003, 2005), Brennecka et al. (2014), Caro et al. (2008), Debaille et al. (2007), and Shih et al. (1982), Symes et al. (2008) and fall to the right of the

1:1 line indicating the bulk meteorites are more depleted in light rare earth elements than their source regions. Note that these data do not define a linear array on this diagram indicating that compositional variation does not reflect simple two-component mixing. Instead, several meteorites with variable $^{147}\text{Sm}/^{144}\text{Nd}$ ratios are derived from source regions with similar $^{147}\text{Sm}/^{144}\text{Nd}$ ratios suggesting that bulk rock chemistry is not related to long-term fractionation of Sm/Nd in the source regions.

Figure 5. A schematic illustration of the early evolution of Mars. The petrogenetic models are based on evidence for a significant metal/silicate segregation event at 4559 ± 8 Ma (Kleine et al., 2004; 2009; Foley et al., 2005; Halliday and Kleine, 2006; Nimmo and Kleine, 2007; Dauphas and Pourmand, 2011), a silicate differentiation of the shergottites source regions occurring at 4504 ± 5 Ma, and thermal modeling that suggest magma ocean solidification occurred rapidly after accretion terminated (Elkins-Tanton, 2008). Option 1 depicts rapid accretion and rapid cooling of the martian magma ocean. It does not account for the young age of silicate differentiation determined for the shergottite source regions, nor provide an obvious mechanism to preserve ^{182}W isotopic differences between various martian meteorites. Option 2 depicts a prolonged period of accretion that is sufficient to extend the period of cooling of some portions of the martian mantle until 4504 Ma. Option 3 depicts rapid initial accretion and magma ocean cooling followed by a giant impact. In this case the silicate differentiation age recorded in the shergottites reflects cooling of a portion of the mantle following melting by the impact event. Both options 2 and 3 imply a significant accretion on Mars for ~ 60 Ma.

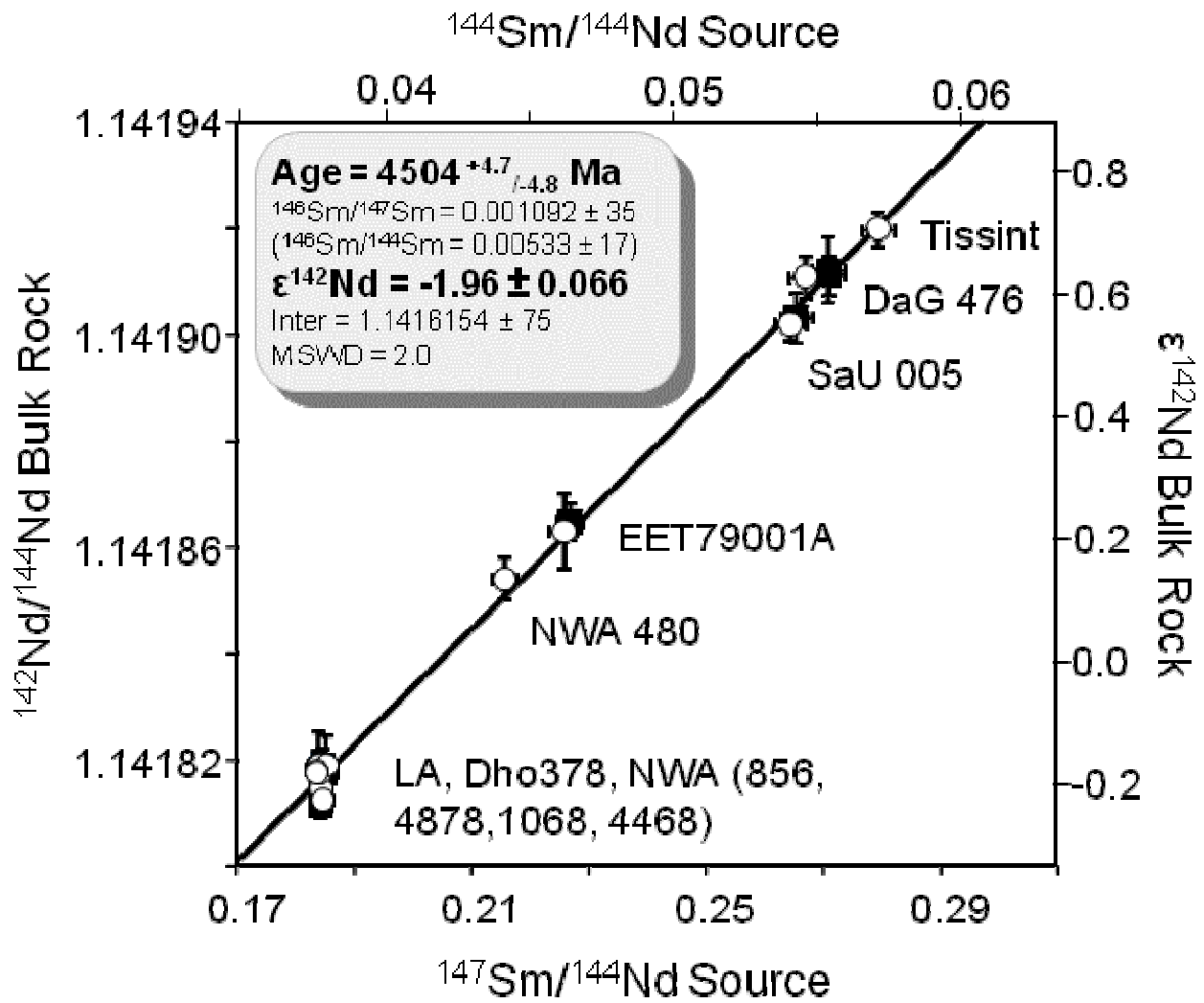


Figure 1

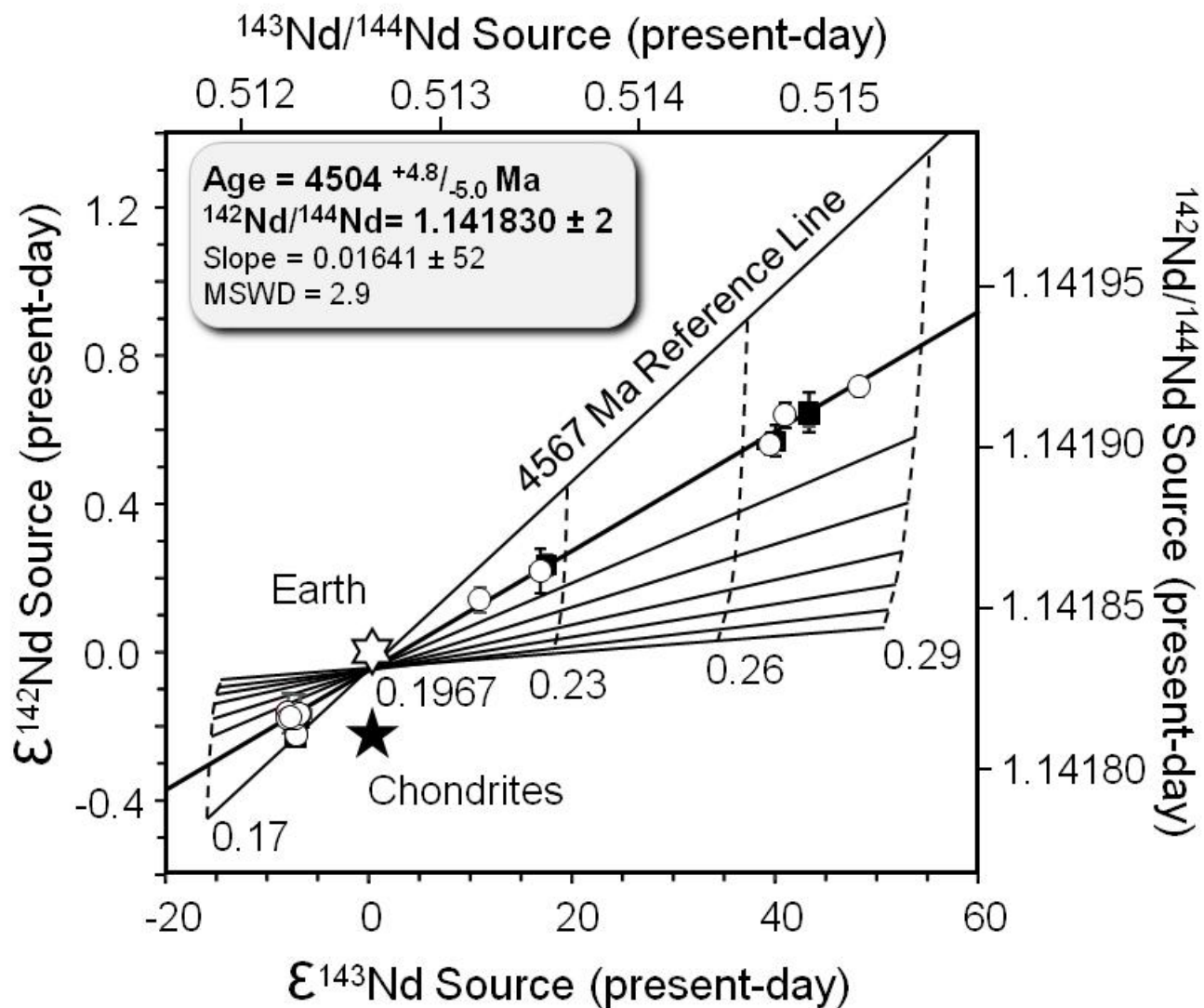


Figure 2

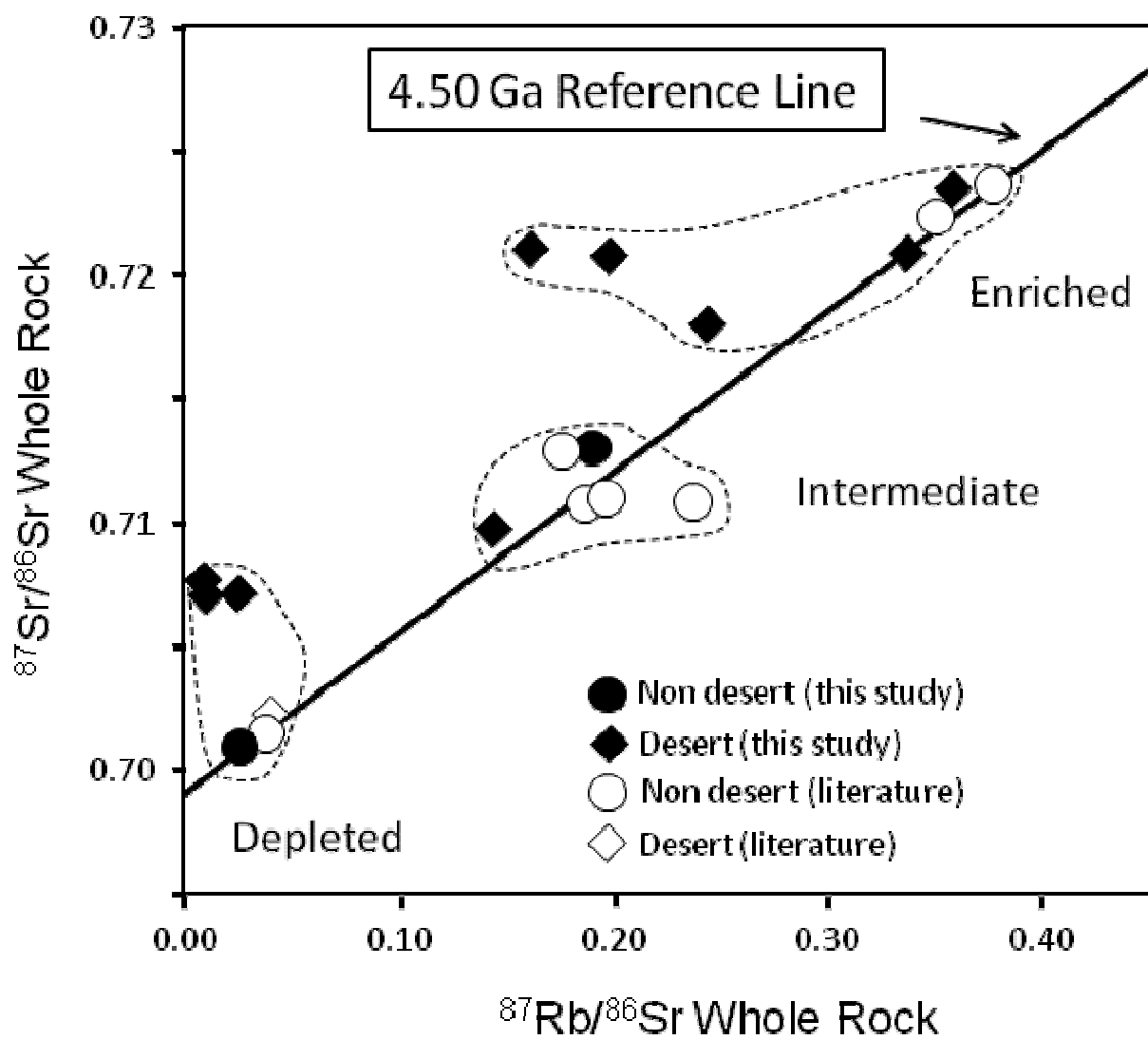


Figure 3

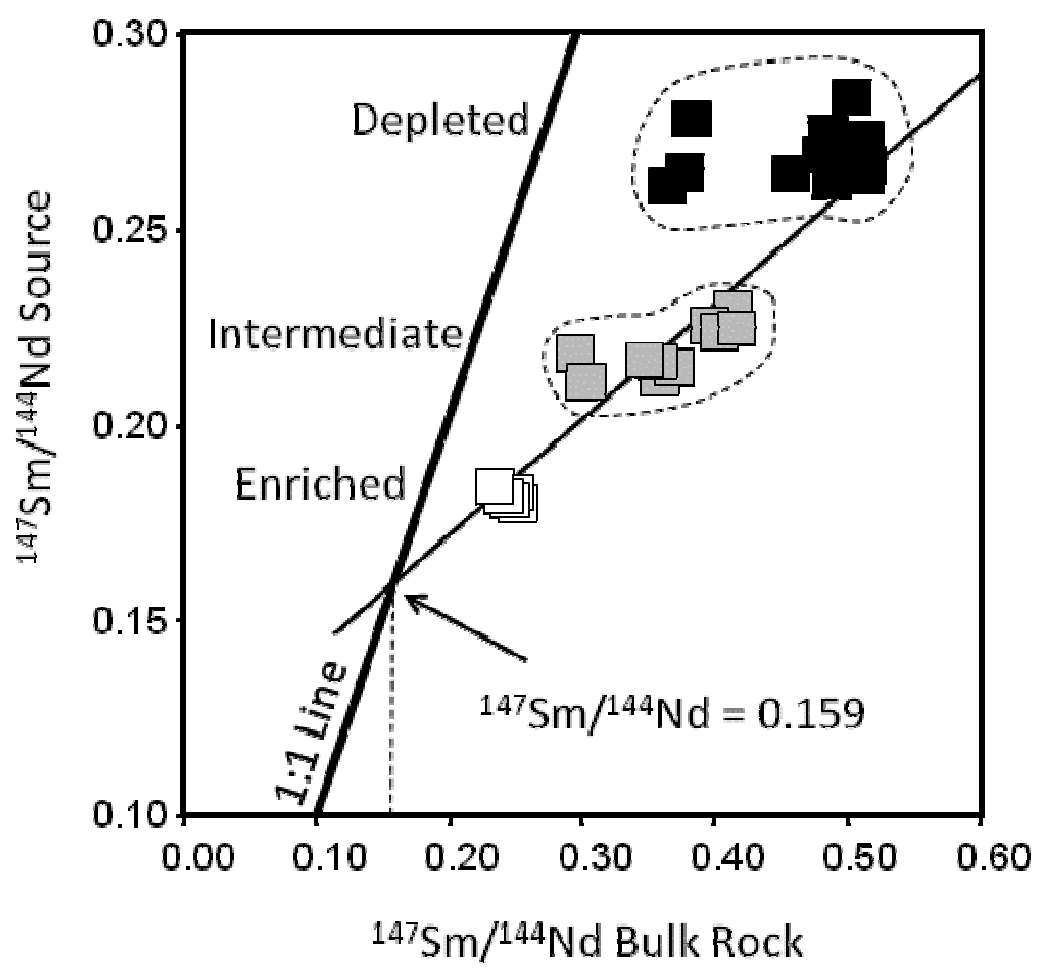


Figure 4

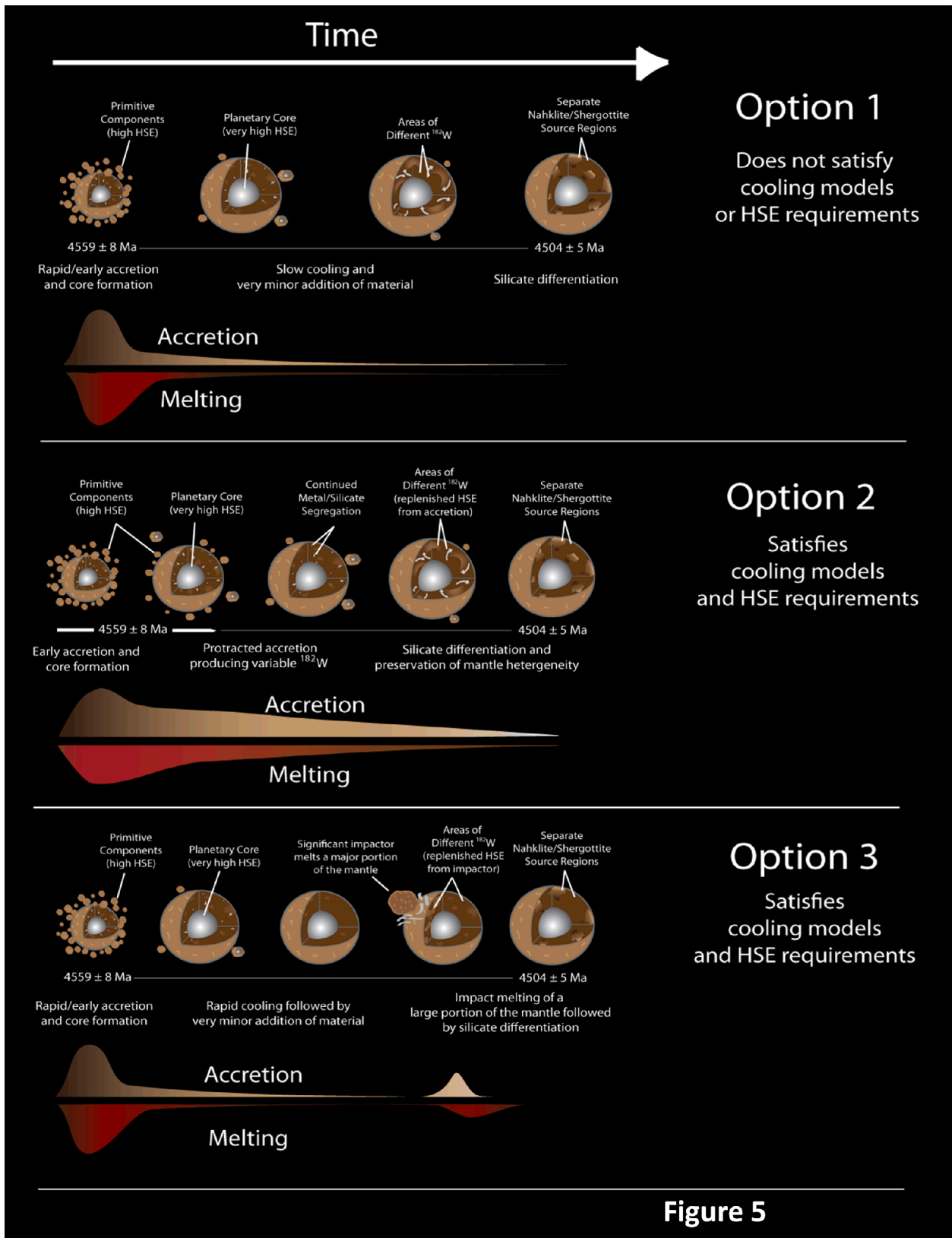


Figure 5